THE IMPACT OF INSECT DEFOLIATION ON A DECEDIOUS FOREST

THE IMPACT OF INSECT DEFOLIATION ON CARBON FLUXES IN A TEMPERATE DECIDUOUS FOREST

By LEJLA LATIFOVIC, B.A.

A Thesis
Submitted to the School of Graduate Studies
in Partial Fulfillment of the Requirements
for the Degree
Master of Science

MASTER OF SCIENCE (2023) McMaster University
(Geography) School of Earth, Environment and Society
Hamilton, Ontario, Canada

TITLE: The Impact of Insect Defoliation on Carbon Fluxes in a Temperate Deciduous Forest

AUTHOR: Lejla Latifovic

Bachelor of Arts (Carleton University, 2009)

SUPERVISOR: M. Altaf Arain

NUMBER OF PAGES: 58

LAY ABSTRACT

Temperate deciduous forests play an important role in carbon sequestration from the atmosphere. However, the impact of climate change, extreme weather, and disturbance events can alter the extent to which these forests sequester carbon, in some cases shifting their role from being a carbon sink to becoming a carbon source to the atmosphere. In 2021, a spongy moth infestation severely defoliated a mature oak-dominated temperate forest north of Lake Erie, Ontario, Canada, turning the forest from a carbon sink to a carbon source. Our analysis indicates that meteorological conditions during the early spring might have influenced the severity of this infestation. Specifically, the prevalence of dry and warm weather conditions enabled the moth to survive and thrive longer. This study shows the significant influence of natural disturbances on forest carbon dynamics as temperatures continue to rise due to climate change. The future role forests play in carbon sequestration will be determined by the severity of disturbance events and the effectiveness of forests to recover in the aftermath of these events.

ABSTRACT

Temperate forests are an important global carbon sink. However, various environmental disturbances can impact carbon sequestration capabilities of these forests. In 2021, a record-breaking defoliation, caused by the spongy moth (*Lymantria dispar L.*, formerly knows as the gypsy moth) occurred in eastern North America. In this study, we assess the impact of this spongy moth defoliation on carbon uptake in a mature oak-dominated temperate forest in the Great Lakes region in Canada, using eddy covariance flux data from 2012 to 2022. The forest is more than 90 years old and known as CA-TPD site in the AmeriFlux and global FLUXNET networks. Study results showed that prior to spongy moth defoliation the forest was a carbon sink with mean annual gross ecosystem productivity (GEP) of 1,367 ± 104, ecosystem respiration (RE) of 1,201 ± 145 and, net ecosystem productivity (NEP) of 197 ± 74 g C m^{-2} yr^{-1} over the 2012–2020 period. However, due the defoliation in the early growing season in 2021, GEP declined to 959 g C m^{-2} yr^{-1} and RE increased to 1,345 g C m^{-2} yr^{-1} causing the forest to became a large source of carbon with annual NEP of -351 g C m^{-2} yr^{-1}. This large decline in annual NEP was a result of both reduced GEP (30%) and elevated RE (12%). However, in 2022, forest carbon fluxes recovered to pre-infestation levels, with a GEP value of 1,671 g C m^{-2} yr^{-1}, an RE value of 1,287 g C m^{-2} yr^{-1}, and an NEP value of 298 g C m^{-2} yr^{-1}, indicating that the forest was once again a large carbon sink. This research demonstrates that major transient natural disturbances such as the 2021 spongy moth defoliation can have a significant impact on forest carbon dynamics in a future warmer climate. The extent to which North American

130 temperate forests will remain a major carbon sink will depend on the severity and intensity
131 of these disturbance events and rate of recovery of forests following the disturbance.

ACKNOWLEDGEMENTS

Dr. Altaf Arain, thank you for giving me this opportunity to come back to school and pursue my passion in climate studies. I am filled with gratitude and appreciation for your guidance, knowledge, support, and time. I am so happy to have had the opportunity to contribute to the important work taking place in the Hydrometeorology and Climatology Group; our collective future will undoubtedly benefit from it.

Elizabeth Arango Ruda, Farbod Tabaei, Tariq Deen, Nur Hussain, and Daniel Mutton I could not have learned as much as I did without your support. Your willingness to share your knowledge with me is something I will always be grateful for. Your comradery made these last two years a lot of fun. Thank you for always being there. Alanna Bodo, thank you for teaching me so much in the few months we had together in the lab. The strong start you provided me with ensured my success. I have been grateful for it on so many occasions.

My mentors. Chris Forrest, Tracy Walden, and John Churchill. Thank you for all that you have shared with me professionally and personally. The opportunities you have created for me and helped me achieve have shaped my career, my decisions, and my future; all for the better. Your belief in me and encouragement fills me with so much gratitude.

To my beautiful parents and sister. You are the epitome of hard work, dedication, and determination. You example is what I strive to follow. Mama (Milica) and tata (Rasim), there are no words that can describe the gratefulness I feel for you; the sacrifices you have made to give us a future that is filled with so much opportunity goes much beyond a thank you. Your unwavering support, encouragement, and the freedom you have granted us to explore our passions means everything to me. Lidija, thank you for taking all my *how-do-I-do-this* calls, I have said it before, and I will say it now, I could not have done this without your support.

To my love, Michael, thank you for all that you do to support me everyday. You make me stronger. To our future baby girl—I can only hope she inherits your boundless patience and profound compassion.

To everyone along the way who had encouraged me to take on this adventure and cheered me on along the way, thank you. I cannot wait to talk all things climate with you.

With immense gratitude, Lejla.

TABLE OF CONTENTS

LAY ABSTRACT iii

ABSTRACT iv

ACKNOWLEDGEMENTS vi

TABLE OF CONTENTS vii

LIST OF FIGURES viii

LIST OF TABLES x

LIST OF ABBREVIATIONS AND SYMBOLS xi

DECLARATION OF ACADEMIC ACHIEVEMENT xii

1. INTRODUCTION 1

    1.1 Background 1

    1.2 Hypothesis and Objectives 4

    1.3 Significance of Study 5

2. METHODS 6

    2.1 Study Site 6

    2.2 Eddy Covariance Flux and Meteorological Measurements 8

    2.3 Growing Season 10

    2.4 Data Processing and Gap-Filling 11

    2.5 Estimates of LAI 13

3. RESULTS 14

    3.1 Meteorological Measurements 14

    3.2 Carbon Fluxes 17

4. DISCUSSION 20

5. CONCLUSIONS 26

6. REFERENCES 28

TABLES 35

FIGURES 39

LIST OF FIGURES

Figure 1 Photos captured at a mature, oak-dominated, deciduous forest part of the Turkey Point Environmental Observatory, north of Lake Erie, Ontario, Canada. Photo A, taken during peak growing season on July 21, 2021, and Photo B, taken on June 15, 2022, illustrate the extend of defoliation experienced in 2021.

Figure 2 Daily time series of mean (a) above, below canopy, and reflected photosynthetically active radiation (PAR), (b) air (Ta) and soil at 5cm depth (Ts) temperature, (c) vapor pressure deficit (VPD), (d) soil moisture (VWC), and (e) precipitation (P) at TPD from 2012–2022.

Figure 3a Mean monthly below canopy photosynthetically active radiation (PAR).

Figure 3b Daily Leaf Area Index (LAI) estimates for TPD from 2012–2022, calculated using the LAI Simple Method as described by Rogers et al. (2021). The plot displays the maximum LAI value for each day.

Figure 4 Daily cumulative precipitation (P) from 2012–2022. Grey shading shows early growing season cumulative precipitation levels. In 2021, there was a noticeable dry period during this time.

Figure 5 Daily sum of total gross ecosystem productivity (GEP), ecosystem respiration (RE), and net ecosystem productivity (NEP) from 2012–2022.

Figure 6 Non-gapfilled, daytime measurements during the growing season, showcasing bin-averaged half-hourly gross ecosystem productivity (GEP) and bin-averaged photosynthetically active radiation (PAR) levels (bin size: 50 µmol m^{-2} s^{-1}) for 2012–2022. The curves represent the fitted hyperbolic model to capture the underlying trend in the data.

224 **Figure 7** Daily cumulative net ecosystem productivity (NEP) at TPD from 2012–
225 2022. A dotted line representing the cumulative NEP at TP39 has been
226 included for comparison. TP39 is a similarly aged forest of different
227 composition which did not experience defoliation by the spongy moth.

228

LIST OF TABLES

Table 1 Growing season (GS) length and number of hot days. The table presents data on the length of the growing season and the number of hot days estimated for each growing season. Hot years are defined as years with an estimated 30 or more hot days, identified as having a daily maximum temperature of 27.5°C or higher. The years considered as hot years in this analysis include 2012, 2016, 2018, 2020, 2021, and 2022.

Table 2 Summary of annual meteorological variables. The table presents data on annual photosynthetically active radiation (PAR), air temperature (Ta), soil temperature at 5cm depth (Ts_{5cm}), vapour pressure deficit (VPD), precipitation (P), and soil moisture ($\theta_{0\text{-}30cm}$ (m^3 m^{-3}). Pre-infestation means (means for meteorological variables between 2012–2020) are given in parentheses.

Table 3 The table presents a summary of annual (A) and growing seasons (GS) gross ecosystem productivity (GEP), ecosystem respiration (RE), and net ecosystem productivity (NEP) flux values. The pre-infestation means (means for fluxes between 2012–2020) are given in parentheses.

Table 4 The relationship between gross ecosystem productivity (GEP) and photosynthetically active radiation (PAR) is illustrated by α, A_{max}, and r^2 values fitted onto the best-fit curve. α signifies the photosynthetic flux per unit of PAR, referred to as quantum yield, while A_{max} represents photosynthetic capacity, also known as the light saturated rate of CO_2 fixation. The goodness of fit for each regression is indicated by the coefficient of determination (r^2).

LIST OF ABBREVIATIONS AND SYMBOLS

C = Carbon

CO_2 = Carbon dioxide

CPEC = Closed-Path Eddy Covariance

EC = Eddy Covariance

Fc = Carbon Flux

GEP = Gross Ecosystem Productivity

IPCC = Intergovernmental Panel on Climate Change

NEE = Net Ecosystem Exchange

NEP = Net Ecosystem Productivity

P = Precipitation

PAR = Photosynthetically Active Radiation

PARd = Downwelling Photosynthetically Active Radiation

RE = Ecosystem Respiration

Ta = Air Temperature

T_{max} = Maximum Temperature

TP39 = Turkey Point 39

TPD = Turkey Point Deciduous

TPEO = Turkey Point Environmental Observatory

Ts = Soil Temperature

VPD = Vapour Pressure Deficit

VWC = Volumetric Water Content

θ = Soil Moisture

DECLARATION OF ACADEMIC ACHIEVEMENT

I, Lejla Latifovic, declare that this thesis titled "THE IMPACT OF INSECT DEFOLIATION ON CARBON FLUXES IN A TEMPERATE DECIDUOUS FOREST" is my own work in collaboration with my supervisor Dr. Altaf Arain.

I, Lejla Latifovic, participated in data collection, conducted data analysis, and drafted the manuscript. Dr. Altaf Arain conceptualized the study, established Turkey Point Environmental Observatory Deciduous Forest flux tower site (CA-TPD), and provided support and guidance at all stages of the research project and write-up.

1. INTRODUCTION

1.1 Background

Concentrations of carbon dioxide (CO_2) in the Earth's atmosphere have increased significantly since the industrial revolution. According to the Intergovernmental Panel on Climate Change (IPCC), the atmospheric concentration of CO_2 in 1750 was about 280 parts per million (ppm). As of 2021, the atmosphere CO_2 concentration increased to about 414 ppm (IPCC, 2021). This increase in CO_2 concentrations has resulted in several significant impacts on the Earth's climate (IPCC, 2021). One of the primary impacts is an increase in global surface temperatures. Since 1850, the average global surface temperature has increased by approximately 1.1°C (IPCC, 2021). This has been a major driver of the changes we are currently seeing in the Earth's climate, hydrologic cycle, and vegetation ecosystems.

Forests play an important role in global carbon sequestration and hence mitigating the impacts of increased atmospheric CO_2 concentrations and climate warming (Canadell & Schulze, 2014; Keenan & Williams, 2018; Waring et al., 2020). Trees and other plants absorb CO_2 from the atmosphere through photosynthesis and store it in live biomass and soil carbon (C) pools for long periods of time (Harris et al., 2021; Sothe et al., 2022). They have the potential to sequester 2.41 Pg C yr^{-1} from the atmosphere (Pan et al., 2011).

Temperate forests which constitute 25% (~10.4 million km^2) of the global forest cover, primarily in eastern North America, Europe, and Asia account for up to 37% of the global forest C uptake (IPCC, 2014; Pan et al., 2011; Tyrrell et al., 2012). Most of the temperate forests are deciduous stands, which cover 7.8 million km^2 of land area across the world

(Allaby, 2006; Vasseur, 2012), with 2.6 million km^2 of these forests located in eastern North America (Commission for Environmental Cooperation, 2006).

Temperate deciduous forests are unique due to their capabilities of sequestering atmospheric CO_2 at high rates because of their rich species composition, large leaf surface area and rootzone, and conducive climatic conditions in which they grow (Beamesderfer et al, 2020; Monson, 2014). Globally, these forests have sequestered 0.72 Pg C yr^{-1} from 1990-2007 (Pan et al., 2011). Additionally, a more recent study by Harris et al. (2021) shows that temperate forests have the capacity to remove approximately 4.4 $GtCO_2e\ yr^{-1}$, accounting for 28% of the global forest greenhouse gas (GHG) removals. Moreover, when considering the global net sink basis, temperate forests contribute to 47% of GHG removals (Harris et al., 2021). However, recent studies indicate that climate change, extreme weather events, and natural and human disturbances may adversely impact the growth and carbon uptake capabilities of temperate deciduous forests, introducing growing uncertainty about the strength of the forest carbon sink (Beamesderfer, 2020; Dale et al., 2001; Hicke et al., 2012; Hurteau, 2021; Li et al., 2023; Reinmann et al., 2019).

There is strong evidence that warmer winter temperatures due to climate change are contributing to more frequent and intense natural disturbances including insect defoliations (Ammunét et al., 2012; Hicke et al., 2012; Williams et al., 2016). Large tracts of forests in western North America in USA and Canada have been infested with mountain pine beetle with very serious implications for forest growth, wood production, and carbon sequestration (Hicke et al., 2013; Hicke et al., 2020; Kurz et al., 2008). It was perceived that perhaps eastern North American forests are less impacted by insect infestation,

336 although there is evidence of mountain pine beetle spreading eastward (Cullingham et al.,
337 2011; Sambaraju et al., 2019). However, in 2021 eastern North American deciduous forests
338 experienced a record-breaking insect infestation and defoliation by the spongy moth
339 (*Lymantria dispar L.*, formerly known as European gypsy moth) that moderately to
340 severely defoliated 1.8 million ha of forest in Southern Ontario, Canada alone (Ontario
341 Ministry of Northern Development, Mines, Natural Resources and Forestry, 2021). This
342 infestation was a progression from previous years where a similar infestation in Ontario in
343 2019 and 2020 impacted 41,600 ha and 569,000 ha of forest, respectively (Ontario Ministry
344 of Northern Development, Mines, Natural Resources and Forestry, 2021). Spongy moth
345 outbreaks are cyclical, occurring every seven to ten years. Previous outbreaks peaked in
346 Ontario in 1985, 1991, 2002, and 2008; however, none reached the intensity of the most
347 recent outbreak in 2021 (Ontario Ministry of Northern Development, Mines, Natural
348 Resources and Forestry, 2021). Figure 1 provides an illustrative example, contrasting the
349 degree of defoliation at TPD in 2021 with 2022 when the forest stand was fully recovered
350 and had a full, normal canopy. The widespread defoliation in 2021 was also reported in
351 northeastern USA impacting 1.05 million ha with roughly half (0.52 million ha) recorded
352 in Michigan State (USDA, 2022).

353 Spongy moth is an invasive and extremely destructive species in North America (Liebhold
354 et al., 1992). Introduced accidentally in 1868 or 1869 by an entomologist in Medford,
355 Massachusetts, USA, it has spread to most of the northeastern states in the USA and eastern
356 provinces in Canada (Leroy et al., 2021; Liebhold et al., 1992). Due to its ability to survive
357 by feeding on a wide variety of deciduous tree species such as Oak, Aspen, Basswood,

Maple, Willow, Hawthorn, Apple, Birch, Alder, and many others (USDA, 2022), and a warmer, more hospitable climate, it is likely that the population will continue to spread across most of the USA and Canada (Régnière et al., 2009), albeit slowly. The moth is an early spring defoliator where early growing season climatic conditions play a key role in the survival, duration, and intensity of the infestation, particularly temperature and moisture (Barbosa et al., 1983; Leonard, 1981; Liebhold et al., 1992). Some studies suggested that early spring drought conditions contribute to increase the length and intensity of the infestation (Addy et al., 2018; Hajek et al., 1996). Increasing wintertime temperatures have been found to improve the survival of overwintering egg masses (Liebhold et al., 1992) while increasing summer temperatures are expanding suitable geographic areas that the moth can inhibit and complete its full lifecycle (Régnière et al., 2009). Given that climate in eastern North America is expected to become warmer and dryer (Arain et al., 2022) it is reasonable to expect the persistence of insect infestations in the future. An experiment performed by Barbosa et al., (1983) also showed that the survival of the spongy moth was greatly dependent on the host plant consumed (shortest lifespans were on pine species and among the longest were on Oaks). Overall spongy moth infestations last for about six weeks (and have been recorded for up to ten weeks) but with devastating consequences for tree foliage, health, and long-term survival of the trees (Leroy et al., 2021; Ward et al., 2022).

1.2 Hypothesis and Objectives

In this study we examined how a spongy moth outbreak early in the growing season in 2021 impacted the carbon sequestration potential of a mature deciduous forest in the Great Lakes region of Ontario, Canada.

Specific objectives of the study were to:

(1) Examine eddy covariance CO_2 fluxes measured in this deciduous forest over an eleven-year period from 2012 and 2022.

(2) Determine the impact of the spongy moth outbreak on net ecosystem productivity (NEP) of the forest.

(3) Investigate how photosynthesis and ecosystem respiration fluxes might have contributed to changes in NEP of the forest during the infestation.

Our hypothesis is that the defoliation caused a large reduction in NEP due to a decrease in photosynthesis that resulted from a severe defoliation of tree species by spongy moth herbivory.

1.3 Significance of Study

This study seeks to contribute insight into the ecological consequences of spongy moth infestations on mature temperate deciduous forests within the Great Lakes Region of Canada. Little research and examination regarding the effects of this specific infestation type, in this region, exists in the literature. To address this gap, our study aims to illustrate the effects by examining carbon fluxes and meteorological patterns both prior to and during the infestation year. Through this investigation, we seek to contribute insight into the underlying mechanisms that could impact the severity of the infestation, as well as the repercussions on forest carbon dynamics throughout the infestation. Subsequently, it is imperative for future research to examine the recovery process of the forest in both the short term (one year) and the mid term (4-5+ years) following this disturbance.

Expanding our understanding of how forests respond to disturbance events will improve our understanding of ecosystem resilience and help scientists illustrate to policymakers the potential role forests can play in mitigating and adapting to future climate change. Moreover, the study will add to the repository of forest carbon data following transient disturbances that can be used in a predictive capacity for future forest management. Simultaneously, this study contributes to the advancement of scientific knowledge by improving our understanding of forest responses, which deepens our understanding of complex natural systems and their interactions.

2. METHODS

2.1 Study Site

Turkey Point Deciduous (42°38′7″N, 80° 33′28″W; 265 m above sea level), hereinafter referred to as TPD site, is part of the Turkey Point Environmental Observatory (TPEO) which includes three different age-sequenced conifer forests (83-, 48-, and 20-year-old as of 2022), a deciduous forest (>90-year old), and an agriculture site located north of Lake Erie in Ontario, Canada, (Arain 2022; Arain et al., 2022). TPEO is part of the Global Water Futures (GWF), AmeriFlux, and global FLUXNET networks. Within these networks TPD site is known as CA-TPD.

Trees at TPD site are about 90-years old (75-to-115-year range) with a mean tree height of 25.7 ± 7.44 m that were naturally regenerated on sandy plains or abandoned agricultural lands in the Lake Erie-Lake Ontario Ecoregion 7E (Crins et al., 2009). This is the most southern forest ecoregion in Ontario and Canada and is home to Canada's largest remaining Carolinian forests (Crins et al., 2009). At TPD site, the dominant tree species is white oak

(*Quercus alba*), and secondary species include red oak (*Quercus rubra*), black oak (*Quercus velutina*), sugar maple (*Acer saccharum*), red maple (*Acer rubrum*), American beech (*Fagus grandifolia*), yellow birch (*Betula alleghaniensis*), white ash (*Fraxinus americana*), and some, roughly 5-10%, conifer species, predominantly white pine (*Pinus strobus*). The understory is composed of a rich diversity of young deciduous trees and plants, including putty root (*Aplectrum hyemale*), yellow mandarin (*Disporum lanuginosum*), Canada mayflower (*Maianthemum canadense*), red trillium (*Trillium erectum*), black cherry (*Prunus serotina*), wood violet (*Viola palmata*), and horsetail (*Equisetum*).

The forest is managed by the Long Point Region Conservation Authority (LPRCA). Prior to 1994 periodic harvesting has taken place in this forest stand. In 1984 and 1986, a commercial harvesting event removed 440 m^3 and 39.97 m^3 of wood volume, respectively. Between 1989 and 1994 harvesting of white pine (106 m^3), red pine (71.42 m^3), poplar (48.22 m^3), and dead oak (61.35 m^3) took place (Beamesderfer et al., 2020).

Soil in the region is predominantly composed of fine-grained sandy glacial deposits with more than 90% sand content (Richard & Hewitt, 2008). Classified in the Canadian System of Soil Classification as Brunisolic Gray-Brown Luvisol, these soils are well-drained and have low water holding capacity (Presant & Acton, 1984). The topography is relatively flat, and the study site is surrounded by agricultural fields. In the early 1900's the area was transformed by forest clearance for agriculture, reducing forest cover from 90% to 11% (Richard & Hewitt, 2008). By mid-19th century reforestation efforts following agriculture abandonment increased forest cover to about 19% (Richard & Hewitt, 2008).

445 The climate of the region is mildest in Canada with cool winters and hot and humid
446 summers; classified by Ecoregions Working Group (1989) in the Humid High Moderate
447 Temperate Ecoclimate Region (Crins et al., 2009). The mean length of the growing season
448 is 217 to 243 days (Crins et al., 2009).

449 **2.2 Eddy Covariance Flux and Meteorological Measurements**

450 Continuous half-hourly flux measurements of energy, water, and carbon dioxide
451 commenced on January 5, 2012, using a closed-path eddy covariance (EC) system (CPEC)
452 following protocols set forth by Fluxnet-Canada and global FLUXNET (Fluxnet-Canada,
453 2003). While measurements continue to present day, this paper considers only those
454 obtained by December 31, 2022. The eddy covariance flux observation system is comprised
455 of a LI-7200 enclosed CO2/H2O infrared gas analyzer (IRGA, Li-COR Inc.) and CSAT3
456 3-D Sonic Anemometer (Campbell Scientific Inc). These sensors are installed on top of a
457 36 m high walk-up scaffolding tower. Eddy covariance fluxes were measured at 20Hz and
458 averaged to half-hourly values using a data computer housed within a field trailer at the
459 base of the tower. IRGA was calibrated for zero and span offsets approximately once a
460 month in the summer and less often in the winter.

461 CO_2 storage flux (the rate of change in CO_2) in the air column below the EC measurement
462 level was calculated by observing the difference between current and previous half-hourly
463 CO_2 concentration measurements at two (mid-canopy and top of tower) heights. A second
464 LI-820 CO2 Gas Analyzer (LI-COR Inc.) was used to sample air at mid-canopy at 16
465 meters height. When mid-canopy measurements were not available the CO_2 storage flux
466 was calculated using the above canopy CO_2 concentration measurements only (36 m). Net

ecosystem exchange (NEE) was calculated as the sum of carbon fluxes (Fc) and the rate of CO_2 storage change in the air column below the EC sensors. Net ecosystem productivity (NEP) was calculated as the inverse of NEE under the convention that negative values of NEE represent uptake of carbon from the atmosphere by the forest (NEP = -NEE). Therefore, positive NEP values indicate carbon sequestration and negative values indicate carbon loss from the forest to the atmosphere.

Air temperature (Ta) and relative humidity (RH) were measured using the HMP155A Temperature and Relative Humidity Probe (Campbell Scientific Inc.). For accuracy and protection from solar radiation interference, the probe is housed within a Compact Aspirated Radiation Shield model 43502-L (R.M. Young Inc.). Horizontal wind speed and direction were measured using a Wind Monitor model 05103 (R.M. Young Inc.). Photosynthetically active radiation (PAR), upwards and downwards, was measured using PQS1 PAR Quantum Sensor (Kipp & Zonen Inc.) while the four components of radiation were measured using CNR4 Net Radiometer (Kipp & Zonen Inc.). Radiation sensors are installed on a metal boom away from the tower to eliminate interference from the support structure. The above-described instruments are all mounted at the top of the scaffolding tower between 35 to 37 meters in height. An additional below canopy PAR sensor (PQS1, Kipp & Zonen Inc.) and a barometric pressure sensor (61302V, R.M. Young Company) measuring atmospheric pressure are installed at the ground. The below canopy PAR sensor measures radiation penetrating the forest canopy at 1.7 m above ground level.

Precipitation (P) data was collected at a location 15 km east of TPD site using an all-weather weighing bucket precipitation gauge (T-200B, GEONOR Inc). A heated tipping bucket rain

gauge (CS700H, Campbell Scientific Inc.) is also installed in a small forest opening about 350 m southwest of the TPD site tower.

Soil temperature (Ts) and soil moisture (θ) were measured using probes at 2, 5, 10, 20, 50, and 100 cm depths in two different soil locations. Ts was measured using 107 Temperature Probe (Campbell Scientific Inc.) and θ using CS650 Soil Water Content Reflectometer (Campbell Scientific Inc.). All data was recorded using multiple data loggers; model CR3000 for meteorological data and model CR10X for precipitation. Automated half-hourly data downloads were conducted, and data saved to the desktop computer housed in the field trailer. Further details of instrumentation are given in Beamesderfer et al. (2020).

2.3 Growing Season

The onset of the growing season was determined as the initial instance when, for five consecutive days, the running daily mean GEP values surpassed the maximum observed growing season GEP by 15% (Chan et al., 2018; Coursolle et al., 2011). Generally, this was during the first two weeks of May each year. The earliest start was May 1 in 2012 and the latest was May 20 in 2014. 2022 had the longest growing season at 170 days. In all other years, the growing season ranged between 149–168 days (Table 1). During this time GEP typically offsets RE and determines the strength of the forest's annual carbon sink. The end of the growing season was determined as the first occurrence when, over a span of five consecutive days, the running daily mean GEP dropped below 15% of the maximum value observed throughout the entire year (Chan et al., 2018; Coursolle et al., 2011). Typically, the growing season concluded between October 15 and October 27.

2.4 Data Processing and Gap-Filling

All data was quality controlled using the Biometeorological Analysis, Collection, and Organizational Node (BACON) software following protocols designed by the Fluxnet-Canada and AmeriFlux Network (Brodeur, 2014). Thresholds were set for all variables using standard values and any data outside of these thresholds was discarded. Data was also manually point cleaned to remove any erroneous spikes the thresholds did not catch.

Within meteorological data, small gaps consisting of a few half-hour periods were linearly interpolated while larger gaps, spanning hours to days, were filled using linear regression model fitted values from other Turkey Point Environmental Observatory sites. The mean flux recovery was 92.5% (ranging from 80% to 98%) over the study period.

The eddy covariance method typically underestimates CO_2 fluxes under calm and stable atmospheric conditions when there is weak turbulent mixing (low friction velocity) such as during calm nights. Distinction between calm and windy conditions was determined using a friction-velocity, u-star threshold (u*) of 0.4 m s^{-1}. Values obtained under this threshold were assumed to be distorted and therefore were rejected and replaced with gap-filling procedures. Employing this method resulted in a mean data capture of 55%; with a range between 47% to 58% over the study period. Gaps were filled using exponential relationships between Ts at 2 cm depth when nighttime NEE was measured at periods when u* > 0.4 m s^{-1}. RE was assumed to be equal to NEE during nighttime (GEP = 0) and daytime when both Ta and Ts are below 0°C. RE was modelled as a function of Ts and $\theta_{0\text{-}30cm}$ according to the following relationship:

$$RE = R_{10} \times Q_{10}^{\frac{T_s-10}{10}} \times f(\theta_{0-30cm}) \quad \text{Eq (1)}$$

where R_{10} and Q_{10} are fitted temperature response parameters that describe the relationship between RE and T_s (Brodeur, 2014). $f(\theta_{0-30cm})$ is a sigmoidal function that characterizes the role of $\theta_{0\text{-}30cm}$ in modifying the temperature response of RE as:

$$f(x) = \frac{1}{[1 + \exp(\theta_1 - \theta_2 x)]} \quad \text{Eq (2)}$$

θ_1 and θ_2 are fitted parameters as a function of the independent variable x, in this case $\theta_{0\text{-}30cm}$, thus acting as a scaling function on the T_s, RE relationship (Brodeur, 2014).

Half-hourly gross ecosystem productivity (GEP) was determined by adding measured NEP to modelled daytime RE. Gaps in GEP were modelled using a rectangular hyperbolic function:

$$GEP = \frac{\alpha PARd\ A_{max}}{\alpha PARd + A_{max}} \times f(T_s) \times f(VPD) \times f(\theta_{0-30cm}) \quad \text{Eq (3)}$$

The first term in the equation defines a Michaelis-Menten relationship between PARd (downwelling photosynthetically active radiation) and GEP, where fitted parameter α is the photosynthetic flux per quanta of PARd (quantum yield) and fitted parameter A_{max} is the photosynthetic capacity. While $f(T_s)$, $f(VPD)$, and $f(\theta_{0-30cm})$ are sigmoidal-type scaling responses of GEP to soil temperature (Ts), vapour pressure deficit (VPD), and soil moisture (θ_{0-30cm}) (Brodeur, 2014).

Gaps in NEP were filled as the difference in modelled GEP and modelled RE. For analysis half-hourly NEP estimates were aggregated to daily, monthly, and annual values. Positive NEP values indicate carbon uptake by the forest and negative values indicate carbon loss to the atmosphere. Annual values were considered as calendar year; however, winter seasonal values were calculated using December values from the previous year with the exception of 2012. Winter season was considered from December of the previous year to January, February, and March of the current year. Spring included April and May. Summer included June, July, August, and September. Autumn included October and November. In addition, hot days were defined as days when daily maximum temperature (T_{max}) $\geq$ 27.5°C, which is the 90th percentile of daily T_{max} over the 30-year reference period (1971–2000) and "hot years" were categorized as the years that had an estimated 30 or more hot days in a given year (Arain et al., 2022). Data processing and analysis was conducted in MATLAB software (The MathWorks Inc.) versions R2019b and R2022b.

2.5 Estimates of LAI

LAI was estimated using the Simple Method as described by Rogers et al. (2021).

$$Le = -\frac{\cos(\theta)}{G(\theta)}\ln\big(P(\theta)\big) \qquad \text{Eq (4)}$$

Briefly, Eq (4) was applied to half hourly above and below canopy PAR measurements to determine the Gap Fraction (P) at a specific Solar Zenith Angle (Θ). Using the Simple Method, we assume leaf angle distribution within the canopy is spherical giving G(Θ) a constant equal to 0.5.

3. RESULTS

3.1 Meteorological Measurements

Daily mean values of PAR, Ta, Ts_{5cm}, VPD, and θ, and daily total values of P are shown in Figure 2. Annual, eleven-year, and pre-infestation mean values for the same variables are give in Table 2. Eleven-year (2012–2022) mean annual PAR at the site was 291 µmol m^{-2}; Ta was 10°C; Ts_{5cm} was 9.7°C; VPD was 0.38 kPa; P was 1,134 mm; and $\theta_{0\text{-}30cm}$ was 0.11 m^3m^{-3}.

The last three years of the study period, 2020 to 2022 had elevated PAR values, where mean annual PAR was above 300 µmol m^{-2} s^{-1}. In all three years, maximum mean daily PAR values exceeded 700 µmol m^{-2} s^{-1} in mid June (June 13, 2020: 714 µmol m^{-2} s^{-1}, June 15, 2021: 739 µmol m^{-2} s^{-1}, June 18, 2022: 789 µmol m^{-2} s^{-1}). In all other years, maximum mean daily PAR did not exceed 650 µmol m^{-2} s^{-1}.

Figure 3a shows below canopy PAR, which steadily increased from February to end of April, when leaves started to emerge at the start of the growing season. Below canopy PAR values began to sharply decline in May, indicating canopy growth, and levelled out by the start of June when canopy is normally fully developed. In 2021, in the early growing season below canopy PAR values were typical with slightly below average values until early May. However, from the start of June in 2021 below canopy PAR rapidly and significantly increased as compared to other years. This increase, measured from 30.69 µmol m^{-2} s^{-1} on May 23, 2021, to 128 µmol m^{-2} s^{-1} on June 13, 2021, signified a more than 300% increase in below canopy PAR within 21 days. The rise in below canopy PAR during a period when one would typically expect canopy closure following leaf emergence suggests a notable

reduction or even the absence of canopy foliage which allowed transmission of radiation to the forest floor (Figure 3a and Figure 2). As a point of comparison, at its June peak below canopy PAR reached 140 µmol m^{-2} s^{-1}, while the greatest peak previously observed was in 2013 with below canopy PAR of 60 µmol m^{-2} s^{-1}. By end of June PAR values were similar to those observed in February, when incoming solar radiation is low. In 2021, below canopy PAR remained high from June to mid October, indicating that canopy had not fully recovered until the end of the growing season. There was no notable deviation in reflected PAR (Figure 2). Compared to other years within the study period, estimates of LAI reveal a notable decline in growing season LAI in 2021, particularly during the month of June. By July, LAI has decreased to a value of 4 m^2 m^{-2}, which is lower than the range observed in previous years (between 4-6 m^2 m^{-2}) (Figure 3b).

The mean temperature at the site during the study period was 10°C, which is 2°C higher than the 30-year mean Ta of 8°C at Environment Canada's Delhi Weather Station. It also slightly exceeded the average established at the site by Beamesderfer et al. (2020) over a five-year (2012–2016) study period by 0.3°C. Overall, six out of the ten years were categorized as "hot" years; characterized by 30 days of greater than 27.5°C daily max temperatures in a given year (Table 1). Five of these six hot years occurred in the most recent seven years of observations (i.e. in 2016, 2018, 2020, 2021, and 2022). 2021 had the second warmest annual average temperature on record. In addition, mean winter temperature was 0°C, and mean June temperature reached a record high of 21.3°C, this was 1.6°C higher than the 10-year mean June Ta of 19.7°C. Soil temperatures at 5cm below ground generally followed air temperature. 2021 had the third highest mean spring Ts_{5cm}

(9.4°C) and the highest summer and autumn Ts_{5cm}, 18.9°C and 11.3°C, respectively. Mean annual Ts_{5cm} was warmest in 2016 (10.7°C). In 2021 mean annual Ts_{5cm} was 10.3°C.

Mean VPD value was 0.38 kPa over the study period. In 2021, there was a notable increase in VPD during the early part of the year and at the start of the growing season, specifically in May. At the same time precipitation was low with virtually no rain recorded during the same month. What followed was an unexpected decrease in VPD from early June to mid-July, which had not been observed during the same period in previous years. By the second half of July, VPD levels had returned to those seen during this time in prior years. $\theta_{0\text{-}30cm}$ had the highest mean annual value of 0.12 $m^3\ m^{-3}$ in 2021. Notably, $\theta_{0\text{-}30cm}$ rose from the middle of June to the middle of July, resulting in mean summertime $\theta_{0\text{-}30cm}$ value of 0.10 $m^3\ m^{-3}$, indicating a higher level of soil moisture than is typical for this time of the year. For comparison, the long-term mean summertime $\theta_{0\text{-}30cm}$ at the site is 0.08 $m^3\ m^{-3}$ while the long-term annual mean for $\theta_{0\text{-}30cm}$ is 0.11 $m^3\ m^{-3}$.

Annual P varied much more from a low annual value of 778 mm in 2016 to a high value of 1,644 mm in 2018. In 2021, annual total P was 1,009 mm. Although, the site experienced lower P during the early part of the year in 2021 (Figure 4), with little to no rain recorded during spring. This dry period was followed by steady rainfall events during the summer, until another dry period was observed in August. Overall, 2021 showed some notable differences in meteorological variables in spring when larvae were feeding on crown foliage. May and June had exceptionally high PAR values, while below canopy PAR values were lowest on record in May and highest on record in June and July. March and April

were warmer compared to previous years, and overall the spring season was unusually warm and dry with higher than usual VPD.

3.2 Carbon Fluxes

Annual dynamics of cumulative daily GEP values are shown in Figure 5. GEP in 2021 displayed considerably lower values compared to all other years in the study period. Specifically, between June 7 and July 14 when GEP remained low with approximately 6 g C m^{-2} d^{-1}. In contrast, during the same period in all previous years, and in 2022, GEP exceeded 10 g C m^{-2} d^{-1}. Even when GEP eventually started to recover in 2021 (mid-July) peak values remained lower than those observed in previous years. However, by the end of the growing season in October, mean monthly GEP was at normal levels compared to all other years. A regression analysis between half hourly PAR and GEP values indicates that GEP increased steadily up to around 800 µmol m^{-2} s^{-1}, beyond which the flux stabilized and began to slightly decline at very high PAR values (e.g. 1,500 µmol m^{-2} s^{-1}) (Figure 6). The same trend was observed in 2021, but at a significantly lower rate due to decreased photosynthetic potential caused by the absence of leaves. For example, in 2021 at PAR value of 800 µmol m^{-2} s^{-1}, GEP was only 11.3 µmol m^{-2} s^{-1}. While, in all other years GEP values ranged from a low of about 14 µmol m^{-2} s^{-1} to a high of 18 µmol m^{-2} s^{-1} (Figure 6). Moreover, photosynthetic capacity (A_{max}) and quantum yield (α) at the site decreased in 2021 from a pre-infestation average of 22.03 µmol m^{-2} s^{-1} to 14.68 µmol m^{-2} s^{-1} and 0.0103 mol CO_2 mol^{-1} to 0.0054 mol CO_2 mol^{-1}, respectively (Table 4).

Daily RE values typically reached peak during the second half of the growing season, anywhere from late July to early September. However, in 2021, while daily peak RE values

were within the range of interannual variation, peak RE was observed earlier in the summer (by end of June) and RE continued to remain high until middle of August (Figure 5).

In 2021, maximum daily NEP value of 4.5 g C m^{-2} d^{-1} was observed on May 31, followed by a continuous decline throughout June, reaching its lowest point on July 8 at daily NEP values of -5.57 g C m^{-2} d^{-1} (Figure 5). By middle of July, NEP began to slowly recover and occasionally surpassed 0 g C m^{-2} d^{-1} for the rest of the growing season. It was unusual to observe daily NEP below 0 g C m^{-2} d^{-1} during peak growing season in the forest. Typically, NEP would increase throughout May, plateau between 6–8 g C m^{-2} d^{-1} in June–July and then gradually decrease during the second half of the growing season (Figure 5).

Dynamics of cumulative daily NEP values showed that prior to the infestation, the forest became a net carbon sink (cumulative NEP > 0) between June 12 (2022) to July 3 (2020) (Figure 7). Then the steady increase in cumulative NEP continued until the end of the growing season. However, early in 2021, cumulative NEP began to trend towards increasingly negative values compared to other years, signaling the forest was not sequestering carbon, rather becoming a larger carbon source by early April. There was a small rebound in NEP from May to early June but after mid-June it continued to trend downward for the rest of the year (Figure 7).

Prior to the spongy moth induced defoliation, the forest had been a moderate to strong carbon sink on an annual basis, where GEP had consistently exceeded RE from 2012 to 2020, and in 2022 (Table 3, Figure 7). Prior to the infestation, mean annual NEP was 197 ± 74 g C m^{-2} yr^{-1}, GEP was 1,367 ± 104 g C m^{-2} yr^{-1}, and RE was 1,201 ± 145 g C m^{-2} yr^{-1}.

However, in 2021, GEP declined to 959 g C m^{-2} yr^{-1} and RE increased to 1,345 g C m^{-2} yr^{-1} resulting in a record-breaking low annual NEP of -351 g C m^{-2} yr^{-1}. After including carbon flux values of the infestation year, mean annual GEP and NEP values declined to 1,327 ± 162 and 142 ± 187 g C m^{-2} yr^{-1}, respectively, while mean annual RE increased to 1,215 ± 144 g C m^{-2} yr^{-1} over the study period (2012–2021) (Table 3, Figure 7).

The infestation event led to an overall decrease in GEP by 408 g C m^{-2} yr^{-1} (30%) compared to pre-infestation mean annual values. Conversely, RE increased by 144 g C m^{-2} yr^{-1} (12%) and this contrast between GEP and RE resulted in a total change in NEP of 548 g C m^{-2} yr^{-1} with the forest being a sink of carbon with mean annual NEP of 197 ± 74 g C m^{-2} yr^{-1} to a source of carbon with mean annual NEP of -351 g C m^{-2} yr^{-1} (279% reduction).

As a point of comparison, a conifer forest of the Turkey Point Environmental Observatory (known as TP39 or CA-TP4 in AmeriFlux and global FLUXNET (Arain, 2018)) with similar age to TPD site was a strong carbon sink in 2021, with annual NEP of 372 g C m^{-2} yr^{-1}, which was the highest annual NEP values observed at this conifer forest since the start of eddy covariance flux measurements in 2003. The predominance of pine trees at TP39 likely meant it experienced minimal, if any, disturbance by the spongy moth. Overall, mean annual NEP at TP39 from 2012 to 2021 was 204 ± 124 g C m^{-2} yr^{-1}, raging from -11 g C m^{-2} yr^{-1} in 2018 to 372 g C m^{-2} yr^{-1} in 2021.

However, in 2022 GEP had a strong recovery. Annual GEP reached 1,671 g C m^{-2} yr^{-1} while RE experienced a slight decrease as compared to 2021, settling at 1,287 g C m^{-2} yr^{-1}. Consequently, there was a substantial rebound in NEP, which reached 298 g C m^{-2} yr^{-1}. The

forest had become a strong carbon sink. This recovery resulted in eleven-year average values of 1,358 ± 186 g C m^{-2} yr^{-1} for GEP, 1,222 ± 138 g C m^{-2} yr^{-1} for RE, and 156 ± 183 g C m^{-2} yr^{-1} for NEP.

Excluding 2021, the mean annual GEP was 1,398 ± 139 g C m^{-2} yr^{-1}, RE was 1,210 ± 137 g C m^{-2} yr^{-1} and NEP was 207 ± 77 g C m^{-2} yr^{-1} over the ten-year non-infestation period.

4. DISCUSSION

In the literature, spongy moth outbreaks have been linked to consecutive years of hot and dry weather conditions (Pernek et al., 2008; Leonard, 1981). High temperatures in the early spring (March) can lead to larvae hatching before budbreak, reducing their survival rates (Williams & Liebhold, 1995) and low temperatures can be fatal to overwintering eggs and larvae. Higher temperatures following timely hatch have been linked to faster growth and development, and increased rates of survival of larvae (Leonard, 1981; Weed et al., 2013). During early spring hatch, heavy precipitation events can cause larvae that have not established feeding sites on foliage to be washed off and drown (Leonard, 1981). Low populations have been correlated with periods of high moisture during early spring (Pernek et al., 2008; Ward et al., 2022).

TPD experienced dry conditions in the early part of 2021 with some of the lowest precipitation levels on record, where no significant rainfall event occurs before late June. Over this period VPD values were also high. These early spring meteorological conditions provided a conducive environment for spongy moth larvae growth and allowed them to establish on leaves before the usual late spring and early summer rain events in the region.

719 The increased survival and accelerated development of the larvae thereby helped to
720 intensify the outbreak. What might be of more significance is that prolonged dry conditions
721 and low moisture in the air limited an entomopathogenic fungus' spore germination and the
722 growth of a nuclear polyhedrosis virus which would have killed the caterpillar before the
723 pupal stage, allowing it to thrive into adulthood (Addy et al., 2018; Hajek et al., 1996;
724 Reilly et al., 2014). It indicates that future changes in precipitation patterns due to climate
725 change might make the fungus, which is a natural control on the infestation, less effective
726 at controlling spongy moth populations in the region (Reilly et al., 2014).

727 In usual circumstances, given warm temperatures and clear skies with high PAR in the
728 spring and summer in 2021, we would have expected GEP to maintain higher values. This
729 expectation aligns with our observations of increased photosynthetic capacity in previous
730 years characterized by high PAR values, such as in 2019, 2020, and 2022. However, in
731 2021, during the early part of the growing season (May and June) the canopy was defoliated
732 by spongy moth herbivory. GEP dropped as photosynthesis was limited due to an absence
733 of leaves. This decline was reflected in reduced photosynthetic capacity, and along with a
734 decrease in estimated LAI, it indicates a loss of leaf area and a reduced capacity for the
735 canopy to perform photosynthesis (GEP).

736 At the same time, RE increased, resulting in a dramatic reduction in annual NEP (-351 g C
737 m^{-2} yr^{-1}), causing the forest to become a source of carbon (Table 3). In the past, the lowest
738 annual NEP was observed in 2015. This year experienced comparable meteorological
739 conditions, a similar start to the growing season, and low early spring precipitation with
740 2021. Despite this, annual GEP in 2015 reached 1,346 g C m^{-2} yr^{-1}, exceeding the 959 g C

741 m^{-2} yr^{-1} recorded in 2021. In 2015, the forest remained a carbon sink with an annual NEP
742 value of 89 g C m^{-2} yr^{-1}. Thus, it is reasonable to assume that, in the absence of the spongy
743 moth attack, the forest would have continued to function as a carbon sink. Given the
744 absence of observable changes in reflected PAR, we can infer that the defoliation of trees
745 by the spongy moth allowed greater light penetration into the understory and forest floor,
746 thereby maintaining some degree of photosynthesis (GEP). It is likely that the understory
747 and coniferous species present at the site were the dominant contributions to GEP during
748 June and early July. This, coupled with development of new leaves, following the end of
749 herbivory, had created opportunities for photosynthetic activity and helped maintain some
750 photosynthetic fluxes during the growing season. The spongy moth defoliation also reduced
751 competition for understory and non-spongy moth feeding trees, which might have
752 potentially contributed to further enhance GEP.

753 Peak defoliation was reached in early July, after which larvae had transformed into pupae,
754 herbivory seized, and leaves started to re-emerge. A shift (reduction) in below canopy PAR
755 values was observed along with a secondary increase in GEP. This was consistent with the
756 literature which describes a secondary flush of canopy and understory leaves once
757 herbivory by the spongy moth is completed (Clark et al., 2010; Hicke et al., 2012; Stephens
758 et al., 2018; Wiley et al., 2017). This secondary canopy growth is supported by stored
759 carbon pools in tree stems and root tissue but comes at a cost to biomass accumulation
760 (Wiley et al., 2017). Despite a resurgence of secondary leaf growth at our site, GEP
761 remained lower than its pre-infestation average. A study by Wiley et al. (2017) found that
762 black oaks, when defoliated, produced smaller leaves in the secondary flush of foliage,

763 which might explain why GEP did not reach typical values following re-foliage. Schäfer et
764 al. (2010) also discovered that only half of the foliage regrew after a complete defoliation
765 by the spongy moth in the Pine Barrens of New Jersey, USA. Therefore, despite an increase
766 in light penetration and reduced competition, herbivory by spongy moth ultimately results
767 in a decrease in overall ecosystem production (Cook et al., 2008). NEP values at our forest
768 site are similar to other deciduous broadleaf forests that have undergone defoliation
769 disturbances, as seen in the data of Clark et al. (2018) and Stephens et al. (2018) and is
770 consistent with a number of studies reviewed by Hicke et al. (2012) which looked at how
771 biotic disturbances impacted forest carbon cycling in Canada and USA.

772 As mentioned earlier, RE showed an increase in 2021. Overall annual RE increased by
773 about 12% (144 g C m^{-2}), and growing season RE increased by about 9% (84 g C m^{-2}) as
774 compared to mean RE values in pre-infestation years. Although, our results supported our
775 hypothesis that defoliation caused a large reduction in NEP due to a decrease in
776 photosynthesis or GEP by 30%, what we also observed was an increase in RE by 12%. The
777 coupling of these two fluxes resulted in a steep decrease in NEP in 2021 by 279% (or -351
778 g C m^{-2} yr^{-1}). This increase in RE is consistent with results reported by Cook et al., (2008)
779 where respiration rates were 6% (45 g C m^{-2}) higher following a forest tent caterpillar
780 defoliation in 2001 at a Chequamegon National Forest in north central Wisconsin, USA.
781 They are also consistent with the findings of Frost and Hunter (2004), who observed an
782 increase in soil respiration following herbivory by the spongy moth in an experiment with
783 red oak saplings. However, not all research sites have observed an increase in RE due to
784 infestation. For example, in an Oak/Pine stand studied by Clark et al. (2010), RE decreased

following full stand defoliation by the spongy moth. Our forest site, while oak dominated, was not completely defoliated. The understory and some secondary tree species had leaves, which means foliar and other autotrophic respiration fluxes were still taking place. It is also possible that heterotrophic respiration, which is impacted by soil temperature and soil moisture, could have increased RE (Clark et al., 2010). This rise in RE in 2021 was within interannual variation, suggesting that meteorological conditions were the likely drivers behind this increase. In fact, RE exhibited elevated levels from the beginning of 2021, which was observed by progressively declining daily cumulative NEP prior to the start of the growing season, and photosynthesis. Prior to leaf-out, NEP is controlled by RE. Growing season RE at our site is predominantly controlled by temperature (Beamesderfer et al., 2020). In 2021, the temperature at our site was among the warmest during the study period, accompanied by mid to late summer precipitation events. Despite the infestation, these factors likely contributed to the observed increase in RE, which, without strong GEP, likely contributed to an even larger observed decrease in NEP.

Overall, RE has shown a slight increasing trend in our forest over the study period. With continued climate warming we would expect this trend to continue. Both, GEP (Keenan et al., 2014) and RE (Barr et al., 2002; Duveneck & Thompson, 2017) have been shown to respond positively to increasing temperatures. However, with warmer temperatures, the potential risk of infestation disturbance is also expected to increase (Williams & Liebhold, 1995). It is important to note that disturbances tend to bolster future RE by increasing the amount of debris on the forest floor and the proportion of dead stem mass to live stem mass (Renninger et al., 2014). According to Renninger et al. (2014) future RE can be impacted

by a lag in the release of carbon from the debris following the disturbance. In their study, annual RE rates from snags and coarse woody debris were 3.5 times larger than pre-disturbance levels four years after a spongy moth defoliation. It will be important to monitor tree vitality, RE, and its impact on overall NEP at TPD in the years to come to fully understand the impact of this record infestation event on the overall carbon balance.

Temperate forests are an important carbon sink (Bonan, 2008) but an increase in disturbance events can counter their effectiveness (Dale et al., 2001). As shown in the literature (Clark et al., 2010; Hicke et al., 2012; Kurz et al., 2008; Williams et al., 2016) insect infestations can strongly impact carbon fluxes rendering the forest a carbon source and these impacts can potentially impact the forest carbon balance in years to come. As the climate continues to change, with warming winters and summers, and changes in precipitation, normal controls on insect outbreaks are being weakened. These include (i) reduced effectiveness of natural enemies like pathogens and viruses that are stunt by dry conditions (Hajek et al., 1996), (ii) increases in herbivory as foliage with higher carbon/nitrogen (C:N) ratio is nutritionally poorer and insect consumption rates go up to compensate or accelerate growth rates and reproduction (Currano et al., 2008; Lindroth et al., 1997) and (iii) shifts in range as new regions become habitable and natural enemies are not present (Régnière et al., 2009) are all contributing to more significant infestations. Given the critical role of forests in global climate policies (IPCC; Paris Agreement, 2015) and given that climate change is likely to create more favourable conditions for increased frequency and intensity of insect infestations in many parts of the world (IPCC, 2021), it is important to continue to gain a better understanding of insect disturbances, the mechanisms

which influence them, and forest responses and recovery processes for future forest planning and management.

5. CONCLUSIONS

In 2021, a record spongy moth infestation was observed in a mature temperate forest located in southern Ontario, Canada, in the Great Lakes Region. Prior to the infestation, the forest was a strong carbon sink with mean annual gross ecosystem productivity (GEP) of 1,367 ± 104, ecosystem respiration (RE) of 1,201 ± 145 and, net ecosystem productivity (NEP) of 197 ± 74 g C m^{-2} yr^{-1} from 2012 to 2020. However, a spongy moth infestation caused GEP to decline to 959 g C m^{-2} yr^{-1} (30% reduction) and during the same time RE had increased to 1,345 g C m^{-2} yr^{-1} (12% increase), resulting in the forest to become a large source of carbon with an annual NEP of -351 g C m^{-2} yr^{-1}. It caused mean annul NEP to decline to 142 ± 187 g C m^{-2} yr^{-1} over the 2012 to 2021 period. The forest became a source of carbon for the first time since the start of eddy covariance flux measurements in 2012. This was despite favourable meteorological conditions and when temperature and precipitation values were within their interannual variations. In contrast, a nearby conifer forest of similar age experienced its highest annual NEP value (372 g C) in 2021 since the start of flux observations in 2003. Our study showed that optimal meteorology conditions, characterized by warmth and dryness, likely contributed to the intensity of the outbreak, enabling the moth to thrive in the absence of natural mortality factors. These findings suggest that spongy moth infestations can transform eastern North American forests from a strong carbon sink to a large carbon source. However, in 2022 the forest had a strong recovery and resumed its role as a carbon sink with an annual NEP of 298 g C m^{-2} yr^{-1}.

Overall, eleven-year (2012 to 2022) annual average GEP was 1,358 ± 186 g C m^{-2} yr^{-1}, RE was 1,222 ± 138 g C m^{-2} yr^{-1}, and NEP was 156 ± 183 g C m^{-2} yr^{-1}. Therefore, it will be important to continue to monitor this forest in the future to assess the long-term impacts of the spongy moth infestation on forest recovery—whether the stand remains a strong carbon sink following disturbance recovery, or if there are long-term impacts that might start to emerge and what those impacts might be. In particular, RE may continue to increase in the coming years as a result of a potential increase in snags and coarse woody debris resulting from the infestation. With a changing climate, insect infestations may become more prevalent in the region with serious consequence for forest carbon balance and their contribution in achieving net zero emission gaols.

This research adds to our understanding of insect infestations in temperate deciduous forests, including factors that can lead to outbreaks and mechanisms that regulate population growth. This information is important for understanding how spongy moth populations may respond to climate change and help inform decisions on climate mitigation strategies using forests ecosystems.

6. REFERENCES

Addy, K., Gold, A. J., Loffredo, J. A., Schroth, A. W., Inamdar, S. P., Bowden, et al. (2018). Stream response to an extreme drought-induced defoliation event. Biogeochemistry, 140(2), 199–215. https://doi.org/10.1007/s10533-018-0485-3

Allaby, M. (2006). *Biomes of the Earth: Temperate forests.* New York, NY: Chelsea House. ISBN-10: 0816053219, ISBN-13: 9780816053216.

Amiro, B. D., Barr, A. G., Barr, J. G., Black, T. A., Bracho, R., Brown, M., et al. (2010). Ecosystem carbon dioxide fluxes after disturbance in forests of North America. *Journal of Geophysical Research*, *115*, G00K02. https://doi.org/10.1029/2010JG001390

Ammunét, T., Kaukoranta, T., Saikkonen, K., Repo, T., & Klemola, T. (2012). Invading and resident defoliators in a changing climate: Cold tolerance and predictions concerning extreme winter cold as a range-limiting factor. *Ecological Entomology, 37*(3), 212–220. https://doi.org/10.1111/j.1365-2311.2012.01358.x

Arain M.A (2018), AmeriFlux CA-TP4 Ontario - Turkey Point 1939 Plantation White Pine, Ver. 4-5, AmeriFlux AMP, (Dataset). https://doi.org/10.17190/AMF/1246012

Arain M.A. (2022). AmeriFlux FLUXNET-1F CA-TPD Ontario - Turkey Point mature deciduous. AmeriFlux (Dataset). https://doi.10.17190/AMF/1881567

Arain, M. A., Xu, B., Brodeur, J. J., Khomik, M., Peichl, M., Beamesderfer, E., Restrepo-Couple, N., & Thorne, R. (2022). Heat and drought impact on carbon exchange in an age-sequence of temperate pine forests. *Ecological Processes*, *11*(1), 7. https://doi.org/10.1186/s13717-021-00349-7

Barbosa, P., Waldvogel, M., Martinat, P., & Douglass, L. W. (1983). Developmental and reproductive performance of the Gypsy Moth, *Lymantria dispar* (L.) (Lepidoptera: Lymantriidae), on selected hosts common to Mid-Atlantic and southern forests. *Environmental Entomology*, *12*(6), 1858–1862. https://doi.org/10.1093/ee/12.6.1858

Barr, A. G., Griffis, T. J., Black, T. A., Lee, X., Staebler, R. M., Fuentes, J. D., Chen, Z., & Morgenstern, K. (2002). Comparing the carbon budgets of boreal and temperate deciduous forest stands. *Canadian Journal of Forest Research, 32*(5), 813–822. https://doi.org/10.1139/x01-131

Beamesderfer, E. R., Arain, M. A., Khomik, M., & Brodeur, J. J. (2020). The impact of seasonal and annual climate variations on the carbon uptake capacity of a deciduous forest within the Great Lakes region of Canada. *Journal of Geophysical Research: Biogeosciences*, *125*(9). https://doi.org/10.1029/2019JG005389

Bonan, G. B. (2008). Forests and climate change: Forcings, feedbacks, and the climate benefits of forests. *Science*, *320*(5882), 1444–1449. https://doi.org/10.1126/science.1155121

Brodeur, J. (2014). Data-driven approaches for sustainable operation and defensible results in a long-term, multi-site ecosystem flux measurement program (Doctoral dissertation). Retrieved from MacSphere. (http://hdl.handle.net/11375/14091). Hamilton, Ontario: McMaster University.

Canadell, J. G., & Schulze, E. D. (2014). Global potential of biospheric carbon management for climate mitigation. *Nature Communications*, *5*(1), 5282. https://doi.org/10.1038/ncomms6282

Chan, F. C. C., Altaf Arain, M., Khomik, M., Brodeur, J. J., Peichl, M., Restrepo-Coupe, N., et al. (2018). Carbon, water and energy exchange dynamics of a young pine plantation forest during the initial fourteen years of growth. *Forest Ecology and Management*, 410, 12–26. https://doi.org/10.1016/j.foreco.2017.12.024

Clark, K., Renninger, H., Skowronski, N., Gallagher, M., & Schäfer, K. (2018). Decadal-scale reduction in forest net ecosystem production following insect defoliation contrasts with short-term impacts of prescribed fires. *Forests*, *9*(3), 145. https://doi.org/10.3390/f9030145

Clark, K. L., Skowronski, N., & Hom, J. (2010). Invasive insects impact forest carbon dynamics. *Global Change Biology*, *16*(1), 88–101. https://doi.org/10.1111/j.1365-2486.2009.01983.x

Commission for Environmental Cooperation. (2006). Ecological regions of North America: Toward a common perspective (Original work published 1997). Montreal, Quebec, Canada: Commission for Environmental Cooperation. http://www.cec.org

Cook, B. D., Bolstad, P. V., Martin, J. G., Heinsch, F. A., Davis, K. J., Wang, W., Desai, A. R., & Teclaw, R. M. (2008). Using light-use and production efficiency models to predict photosynthesis and net carbon exchange during forest canopy disturbance. *Ecosystems*, *11*(1), 26–44. https://doi.org/10.1007/s10021-007-9105-0

Coursolle, C., Margolis, H. A., Giasson, M.-A., Bernier, P.-Y., Amiro, B. D., Arain, M. A., et al. (2012). Influence of stand age on the magnitude and seasonality of carbon fluxes in Canadian forests. *Agricultural and Forest Meteorology*, 165, 136–148. https://doi.org/10.1016/j.agrformet.2012.06.011

Cullingham, C.I., Cooke, J.E., Dang, S., Davis, C.S., Cooke, B.J., & Coltman, D.W. (2011). Mountain pine beetle host-range expansion threatens the boreal forest. *Molecular Ecology*, *20*(10), 2157–2171. https://doi.org/10.1111/j.1365-294X.2011.05086.x

Currano, E. D., Wilf, P., Wing, S. L., Labandeira, C. C., Lovelock, E. C., & Royer, D. L. (2008). Sharply increased insect herbivory during the Paleocene–Eocene Thermal Maximum. *Proceedings of the National Academy of Sciences, 105*(6), 1960–1964. https://doi.org/10.1073/pnas.0708646105

Crins, W. J., Gray, P. A., Uhlig, P. W. C., & Wester, M. C. (2009). The ecosystems of Ontario, part 1: Ecozones and ecoregions. *Ontario Ministry of Natural Resources, Science & Information Branch, Inventory, Monitoring and Assessment Section.* Retrieved from https://www.ontario.ca/page/ecosystems-ontario-part-1-ecozones-and-ecoregions

Dale, V. H., Joyce, L. A., Mcnulty, S., Neilson, R. P., Ayres, M. P., Flannigan, et al. (2001). Climate change and forest disturbances. *BioScience*, *51*(9), 723. https://doi.org/10.1641/0006-3568(2001)051[0723:CCAFD]2.0.CO;2

Duveneck, M. J., & Thompson, J. R. (2017). Climate change imposes phenological trade-offs on forest net primary productivity. *Journal of Geophysical Research: Biogeosciences, 122*(9), 2298–2313. https://doi.org/10.1002/2017JG004025

Flower, C. E., & Gonzalez-Meler, M. A. (2015). Responses of temperate forest productivity to insect and pathogen disturbances. *Annual Review of Plant Biology*, *66*(1), 547–569. https://doi.org/10.1146/annurev-arplant-043014-115540

Fluxnet-Canada, 2003. Fluxnet-Canada Measurement Protocols.

Frost, C. J., & Hunter, M. D. (2004). Insect canopy herbivory and frass deposition affect soil nutrient dynamics and export in oak mesocosms. *Ecology*, *85*(12), 3335–3347. https://doi.org/10.1890/04-0003

Gallinat, A. S., Primack, R. B., & Wagner, D. L. (2015). Autumn, the neglected season in climate change research. *Trends in Ecology & Evolution*, *30*(3), 169–176. https://doi.org/10.1016/j.tree.2015.01.004

Harris, N. L., Gibbs, D. A., Baccini, A., Birdsey, R. A., De Bruin, S., Farina, M., et al. (2021). Global maps of twenty-first century forest carbon fluxes. *Nature Climate Change*, *11*(3), 234–240. https://doi.org/10.1038/s41558-020-00976-6

Hajek, A. E., Elkinton, S., & Witcosky, J. (1996). Introduction and spread of the fungal pathogen *Entomophaga maimaiga* (Zygomycetes: Entomophthorales) along the leading edge of Gypsy Moth (Lepidoptera: Lymantriidae) spread. *Environmental Entomology*, *25*(5), 1235–1247. https://doi.org/10.1093/ee/25.5.1235

Heimann, M., & Reichstein, M. (2008). Terrestrial ecosystem carbon dynamics and climate feedbacks. *Nature*, *451*(7176), 289–292. https://doi.org/10.1038/nature06591

Hicke, J. A., Allen, C. D., Desai, A. R., Dietze, M. C., Hall, R. J., Hogg, E. H., et al. (2012). Effects of biotic disturbances on forest carbon cycling in the United States and Canada. *Global Change Biology*, *18*(1), 7–34. https://doi.org/10.1111/j.1365-2486.2011.02543.x

Hicke, J. A., Meddens, A. J. H., Allen, C. D., & Kolden, C. A. (2013). Carbon stocks of trees killed by bark beetles and wildfire in the western United States. *Environmental Research Letters*, 8(3), doi:10.1088/1748-9326/8/3/035032

Hicke, J. A., Xu, B., Meddens, A. J. H., & Egan, J. M. (2020). Characterizing recent bark beetle-caused tree mortality in the western United States from aerial surveys. *Forest Ecology and Management, 475*, 118402. https://doi.org/10.1016/j.foreco.2020.118402

Hurteau, M. D. (2021). The role of forests in the carbon cycle and in climate change. In T. M. Letcher (Eds.), *Climate Change, Third Edition* (pp. 561–579). Elsevier B.V. https://doi.org/10.1016/B978-0-12-821575-3.00027-X

IPCC (2014). In C. B. Field, et al. (Eds.), Terrestrial and inland water systems. *In: Climate change 2014: Impacts, adaptation, and vulnerability. Part A: Global and sectoral aspects. Contribution of Working Group II to the Fifth Assessment Report of the Intergovernmental Panel on Climate Change* (pp. 271–359). Cambridge University Press, Cambridge, United Kingdom and New York, NY, USA.

IPCC (2021). In V. Masson-Delmotte, et al. (Eds.), *Climate Change 2021: The physical science basis. Contribution of Working Group I to the Sixth Assessment Report of the Intergovernmental Panel on Climate Change*. Cambridge University Press, Cambridge, United Kingdom and New York, NY, USA.

Keenan, T. F., Gray, J., Friedl, M. A., Toomey, M., Bohrer, G., Hollinger, D. Y., et al. (2014). Net carbon uptake has increased through warming-induced changes in temperate forest phenology. *Nature Climate Change, 4*(7), 598–604. https://doi.org/10.1038/nclimate2253

Keenan, T. F., & Williams, C. A. (2018). The terrestrial carbon sink. *Annual Review of Environment and Resources, 43*(1), 219–243. https://doi.org/10.1146/annurev-environ-102017-030204

Kurz, W. A., Dymond, C. C., Stinson, G., Rampley, G. J., Neilson, E. T., Carroll, A. L., Ebata, T., & Safranyik, L. (2008). Mountain pine beetle and forest carbon feedback to climate change. *Nature*, *452*(7190), 987–990. https://doi.org/10.1038/nature06777

Leonard, D. E. (1981). Chapter 2: Bioecology of the Gypsy Moth. In C.C. Doane, M.L. McManus (Eds), *The Gypsy Moth: Research toward integrated pest management* (pp. 9–29). Washington, DC: U. S. Department of Agriculture. Retrieved from ttps://handle.nal.usda.gov/10113/CAT82474520

Leroy, B. M. L., Lemme, H., Braumiller, P., Hilmers, T., Jacobs, M., Hochrein, S., et al. (2021). Relative impacts of gypsy moth outbreaks and insecticide treatments on forest resources and ecosystems: An experimental approach. *Ecological Solutions and Evidence, 2*(1). https://doi.org/10.1002/2688-8319.12045

Li, Y., Zhang, W., Schwalm, C. R., Gentine, P., Smith, W. K., Ciais, P., et al. (2023). Widespread spring phenology effects on drought recovery of northern hemisphere ecosystems. *Nature Climate Change, 13*(2), 182–188. https://doi.org/10.1038/s41558-022-01584-2

Liebhold, A. M., Halverson, J. A., & Elmes, G. A. (1992). Gypsy Moth invasion in North America: A quantitative analysis. *Journal of Biogeography*, *19*(5), 513. https://doi.org/10.2307/2845770

Lindroth, R. L., Klein, K. A., Hemming, Jocel. D. C., & Feuker, A. M. (1997). Variation in temperature and dietary nitrogen affect performance of the gypsy moth (Lymantria dispar L.). *Physiological Entomology*, *22*(1), 55–64. https://doi.org/10.1111/j.1365-3032.1997.tb01140.x

Medvigy, D., Clark, K. L., Skowronski, N. S., & Schäfer, K. V. R. (2012). Simulated impacts of insect defoliation on forest carbon dynamics. *Environmental Research Letters*, *7*(4), 045703. https://doi.org/10.1088/1748-9326/7/4/045703

Monson, R. K. (2014). Ecology of temperate forests. In R. K. Monson, M. Tester, R. Jorgensen (Eds.), *Ecology and the Environment. The Plant Sciences* (Vol 8, pp. 273–296). New York, NY: Springer. https://doi.org/10.1007/978-1-4614-7501-9_5

Morgenstern, K., Black, T. A., Humphreys, E. R., Griffis, T. J., Drewitt, G. B., Cai, T., et al. (2004). Sensitivity and uncertainty of the carbon balance of a Pacific Northwest Douglas-fir forest during an El Niño/La Niña cycle. *Agricultural and Forest Meteorology*, *123*(3–4), 201–219. https://doi.org/10.1016/j.agrformet.2003.12.003

Ontario Ministry of Northern Development, Mines, Natural Resources and Forestry. (2021). *Forest Health Conditions in Ontario 2021*. Science and Research Branch. https://www.ontario.ca/page/forest-health-conditions

Pan, Y., Birdsey, R. A., Fang, J., Houghton, R., Kauppi, P. E., Kurz, W. A., et al. (2011). A large and persistent carbon sink in the world's forests. *Science*, *333*(6045), 988–993. https://doi.org/10.1126/science.1201609

Pernek, M., Pilas, I., Vrbek, B., Benko, M., Hrasovec, B., & Milkovic, J. (2008). Forecasting the impact of the Gypsy moth on lowland hardwood forests by analyzing the cyclical pattern of population and climate data series. *Forest Ecology and Management*, *255*(5–6), 1740–1748. https://doi.org/10.1016/j.foreco.2007.11.031

Presant, E. W., & Acton, C. J. (1984). The soils of the regional municipality of Haldimand-Norfolk. Ontario Institute of Pedology, Ontario Ministry of Agriculture and Food. Report no. 57, Vol 2. Retrieved from https://www.worldcat.org/title/soils-of-the-regionalmunicipality-of-haldimand-norfolk/oclc/630077090

Régnière, J., Nealis, V., & Porter, K. (2009). Climate suitability and management of the gypsy moth invasion into Canada. *Biological Invasions*, *11*(1), 135–148. https://doi.org/10.1007/s10530-008-9325-z

Reilly, J. R., Hajek, A. E., Liebhold, A. M., & Plymale, R. (2014). Impact of Entomophaga maimaiga (Entomophthorales: Entomophthoraceae) on outbreak Gypsy Moth populations (Lepidoptera: Erebidae): The role of weather. *Environmental Entomology*, 43(3), 632–641. https://doi.org/10.1603/EN13194

Reinmann, A. B., Susser, J. R., Demaria, E. M. C., & Templer, P. H. (2019). Declines in northern forest tree growth following snowpack decline and soil freezing. *Global Change Biology*, *25*(2), 420–430. https://doi.org/10.1111/gcb.14420

Renninger, H. J., Carlo, N., Clark, K. L., & Schäfer, K. V. R. (2014). Modeling respiration from snags and coarse woody debris before and after an invasive gypsy moth disturbance. *Journal of Geophysical Research: Biogeosciences*, *119*(4), 630–644. https://doi.org/10.1002/2013JG002542

Richart, M., & Hewitt, N. (2008). Forest Remnants in the Long Point Region, Southern Ontario: Tree species diversity and size structure. *Landscape and Urban Planning*, *86*(1), 25–37. https://doi.org/10.1016/j.landurbplan.2007.12.005

Rogers, C., Chen, J. M., Croft, H., Gonsamo, A., Luo, X., Bartlett, P., & Staebler, R. M. (2021). Daily leaf area index from photosynthetically active radiation for long term records of canopy structure and leaf phenology. *Agricultural and Forest Meteorology*, 304–305, 108407. https://doi.org/10.1016/j.agrformet.2021.108407

Sambaraju, K. R., Carroll, A. L., & Aukema, B. H. (2019). Multiyear weather anomalies associated with range shifts by the mountain pine beetle preceding large epidemics. *Forest Ecology and Management*, *438*, 86–95. https://doi.org/10.1016/j.foreco.2019.02.011

Schäfer, K. V. R., Clark, K. L., Skowronski, N., & Hamerlynck, E. P. (2010). Impact of insect defoliation on forest carbon balance as assessed with a canopy assimilation model. *Global Change Biology*, *16*(2), 546–560. https://doi.org/10.1111/j.1365-2486.2009.02037.x

Schindlbacher, A., Wunderlich, S., Borken, W., Kitzler, B., Zechmeister-Boltenstern, S., & Jandl, R. (2012). Soil respiration under climate change: Prolonged summer drought offsets soil warming effects. *Global Change Biology*, *18*(7), 2270–2279. https://doi.org/10.1111/j.1365-2486.2012.02696.x

Stephens, J. J., Black, T. A., Jassal, R. S., Nesic, Z., Grant, N. J., Barr, A. G., et al. (2018). Effects of forest tent caterpillar defoliation on carbon and water fluxes in a boreal aspen stand. *Agricultural and Forest Meteorology*, *253–254*, 176–189. https://doi.org/10.1016/j.agrformet.2018.01.035

Sothe, C., Gonsamo, A., Arabian, J., Kurz, W. A., Finkelstein, S. A., & Snider, J. (2022). Large soil carbon storage in terrestrial ecosystems of Canada. *Global Biogeochemical Cycles*, *36*(2). https://doi.org/10.1029/2021GB007213

Tyrrell, M. L., Ross, J., & Kelty, M. (2012). Carbon dynamics in the temperate forest. In M. S. Ashton, M. L. Tyrrell, D. Spalding, & B. Gentry (Eds.), *Managing forest carbon in a changing climate* (pp. 77–107). Dordrecht, Netherlands: Springer Science & Business Media. https://doi.org/10.1007/978-94-007-2232-3_5

United Nations Framework Convention on Climate Change. (2015). Paris Agreement. Retrieved from https://unfccc.int/process-and-meetings/the-paris-agreement/the-paris-agreement

United States Department of Agriculture, Forest Services, Eastern Region State and Private Forestry. (2022). *Eastern Region Forest Health Conditions Report 2021*. Retrieved from https://www.fs.usda.gov/foresthealth/publications/fhp/index.shtml

Vasseur, L. (2012). Restoration of deciduous forests. *Nature Education Knowledge, 3*(12), 1.

Ward, J. S., Jones, C. C., & Barsky, J. P. (2022). Multiyear defoliations in southern New England increases oak mortality. *Canadian Journal of Forest Research, 52*(2), 269–279. https://doi.org/10.1139/cjfr-2021-0174

Waring, B., Neumann, M., Prentice, I. C., Adams, M., Smith, P., & Siegert, M. (2020). Forests and decarbonization – Roles of natural and planted forests. *Frontiers in Forests and Global Change*, 3. https://doi.org/10.3389/ffgc.2020.00058

Weed, A. S., Ayres, M. P., & Hicke, J. A. (2013). Consequences of climate change for biotic disturbances in North American forests. *Ecological Monographs, 83*(4), 441–470. https://doi.org/10.1890/13-0160.1

Wiley, E., Casper, B. B., & Helliker, B. R. (2017). Recovery following defoliation involves shifts in allocation that favour storage and reproduction over radial growth in black oak. *Journal of Ecology*, *105*(2), 412–424. https://doi.org/10.1111/1365-2745.12672

Williams, D. W., & Liebhold, A. M. (1995). Herbivorous insects and global change: Potential changes in the spatial distribution of forest defoliator outbreaks. *Journal of Biogeography*, *22*(4/5), 665. https://doi.org/10.2307/2845968

Williams, C. A., Gu, H., MacLean, R., Masek, J. G., & Collatz, G. J. (2016). Disturbance and the carbon balance of US forests: A quantitative review of impacts from harvests, fires, insects, and droughts. *Global and Planetary Change, 143*, 66–80. https://doi.org/10.1016/j.gloplacha.2016.06.002

TABLES

Table 1: Growing season (GS) length and number of hot days. The table presents data on the length of the growing season and the number of hot days estimated for each growing season. Hot years are defined as years with an estimated 30 or more hot days, identified as having a daily maximum temperature of 27.5°C or higher. The years considered as hot years in this analysis include 2012, 2016, 2018, 2020, 2021, and 2022.

	2012	**2013**	**2014**	**2015**	**2016**	**2017**	**2018**	**2019**	**2020**	**2021**	**2022**
GS Start	01-May	07-May	20-May	07-May	17-May	15-May	14-May	19-May	16-May	13-May	10-May
GS End	15-Oct	15-Oct	15-Oct	18-Oct	27-Oct	26-Oct	22-Oct	17-Oct	19-Oct	25-Oct	26-Oct
Length (in days)	168	162	149	165	164	165	162	162	157	166	170
Number of hot days	73	19	8	15	35	20	48	19	40	39	31

Table 2. Summary statistics for annual meteorological variables. The table presents data on annual photosynthetically active radiation (PAR), air temperature (Ta), soil temperature at 5cm depth (Ts_{5cm}), vapour pressure deficit (VPD), precipitation (P), and soil moisture ($\theta_{0\text{-}30cm}$). Pre-infestation means (means for meteorological variables between 2012–2020) are given in parentheses.

	2012	**2013**	**2014**	**2015**	**2016**	**2017**	**2018**	**2019**	**2020**	**2021**	**2022**	**11-year mean**
PAR ($\mu mol\ m^{-2}$)	287	267	280	285	287	270	266	276	317	321	343	291 (282)
Mean Ta (°C)	11.8	9.2	8.0	9.2	10.6	10.0	9.7	9.1	10.6	11.3	10.3	10 (9.8)
Mean Ts_{5cm} (°C)	10.4	9.2	8.8	9.8	10.7	10.0	9.5	9.2	9.7	10.3	9.6	9.7 (9.7)
Mean VPD (kPa)	0.57	0.35	0.33	0.35	0.42	0.36	0.33	0.29	0.37	0.38	0.38	0.38 (0.38)
Total P (mm)	1001	1266	1429	811	778	1153	1644	1126	1127	1009	960	1118 (1148)
$\theta_{0\text{-}30cm}$ ($m^3\ m^{-3}$)	0.10	0.11	0.11	0.10	0.09	0.10	0.11	0.11	0.11	0.12	0.11	0.11 (0.11)

Table 3. The table presents a summary of annual (A) and growing seasons (GS) gross ecosystem productivity (GEP), ecosystem respiration (RE), and net ecosystem productivity (NEP) flux values. The pre-infestation means (means for fluxes between 2012–2020) are given in parentheses.

		2012	**2013**	**2014**	**2015**	**2016**	**2017**	**2018**	**2019**	**2020**	**2021**	**2022**	**11-year mean**
GEP ($g\ C\ m^{-2}\ yr^{-1}$)	A	1123	1387	1382	1346	1417	1441	1316	1484	1412	959	1671	1358 (1367)
	GS	1070	1335	1335	1307	1365	1387	1267	1434	1356	928	1588	1307 (1317)
RE ($g\ C\ m^{-2}\ yr^{-1}$)	A	860	1279	1120	1282	1250	1316	1144	1250	1306	1345	1287	1222 (1201)
	GS	599	1049	892	1021	959	1031	913	1000	959	1020	1075	956 (936)
NEP ($g\ C\ m^{-2}\ yr^{-1}$)	A	310	143	294	89	192	165	189	251	142	-351	298	156 (197)
	GS	475	286	442	277	402	357	343	428	392	-116	497	344 (378)

Table 4. The relationship between gross ecosystem productivity (GEP) and photosynthetically active radiation (PAR) is illustrated by α, A_{max}, and r^2 values fitted onto the best-fit curve. α signifies the photosynthetic flux per unit of PAR, referred to as quantum yield, while A_{max} represents photosynthetic capacity, also known as the light saturated rate of CO_2 fixation. The goodness of fit for each regression is indicated by the coefficient of determination (r^2).

Year	α	A_{max}	r^2
2012	0.0084	19.39	0.95
2013	0.0103	21.44	0.92
2014	0.0106	22.19	0.90
2015	0.0098	21.58	0.89
2016	0.0096	20.83	0.87
2017	0.0112	23.51	0.93
2018	0.0099	20.59	0.87
2019	0.0124	25.61	0.94
2020	0.0102	23.11	0.93
2021	0.0054	14.68	0.81
2022	0.0099	24.80	0.92

FIGURES

Photo A Photo B

Figure 1. Photos captured at a mature, oak-dominated, deciduous forest part of the Turkey Point Environmental Observatory, north of Lake Erie, Ontario, Canada. Photo A, taken during peak growing season on July 21, 2021, and Photo B, taken on June 15, 2022, illustrate the extend of defoliation experienced in 2021.

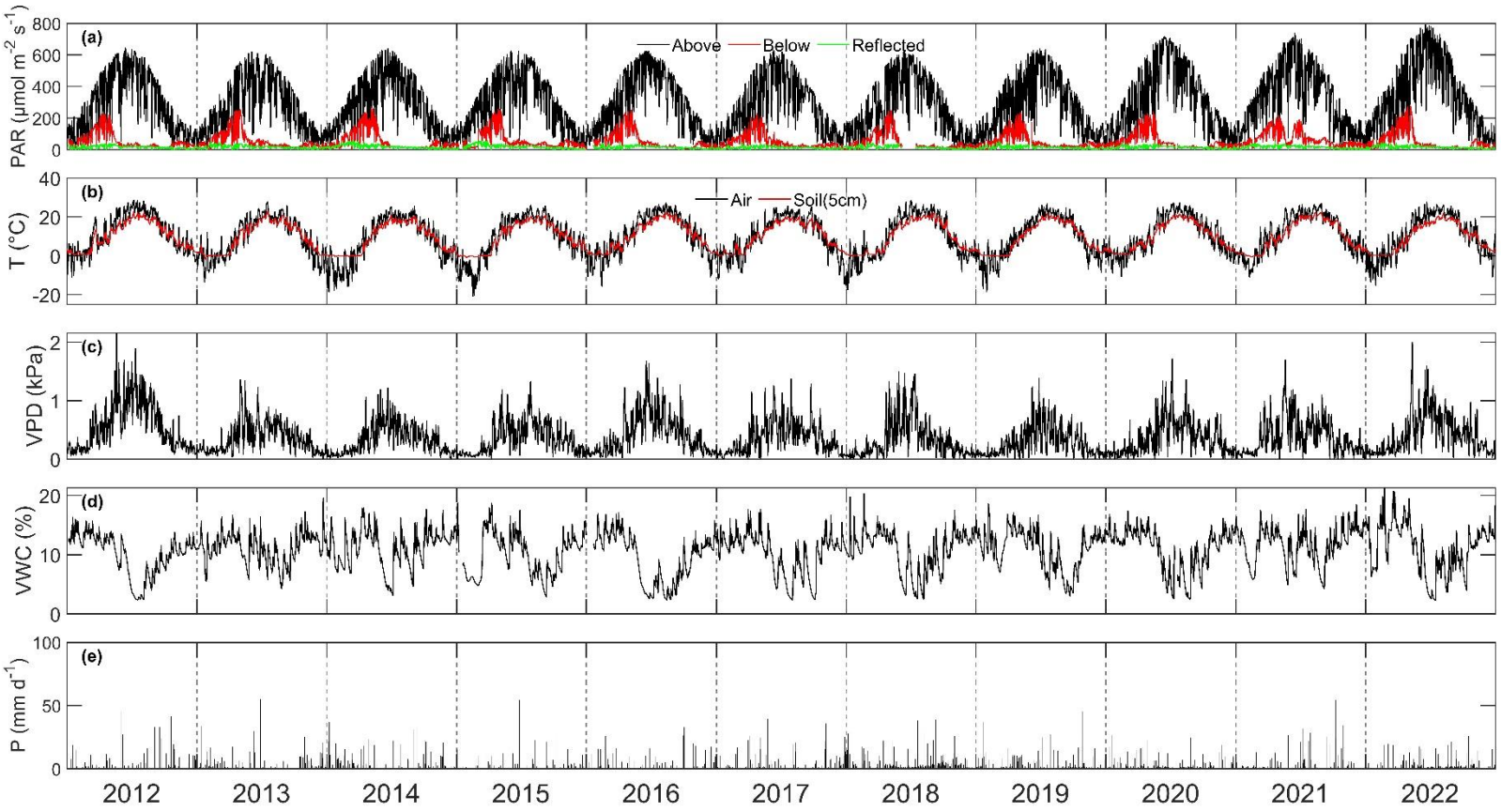

Figure 2. Daily time series of mean (a) above, below canopy, and reflected photosynthetically active radiation (PAR), (b) air (Ta) and soil at 5cm depth (Ts) temperature, (c) vapor pressure deficit (VPD), (d) soil moisture (VWC), and (e) precipitation (P) at TPD from 2012–2022.

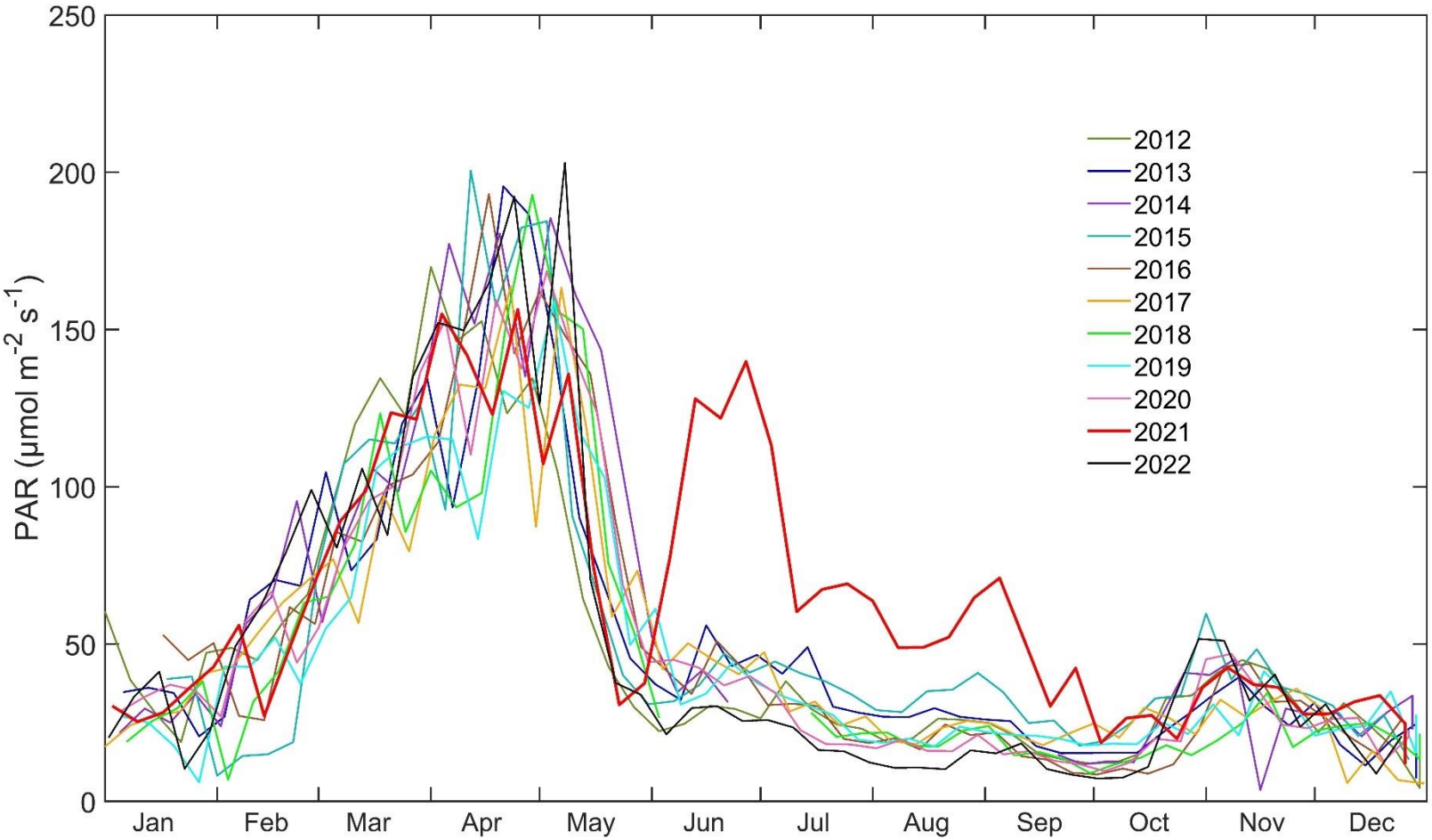

Figure 3a. Mean monthly below canopy photosynthetically active radiation (PAR).

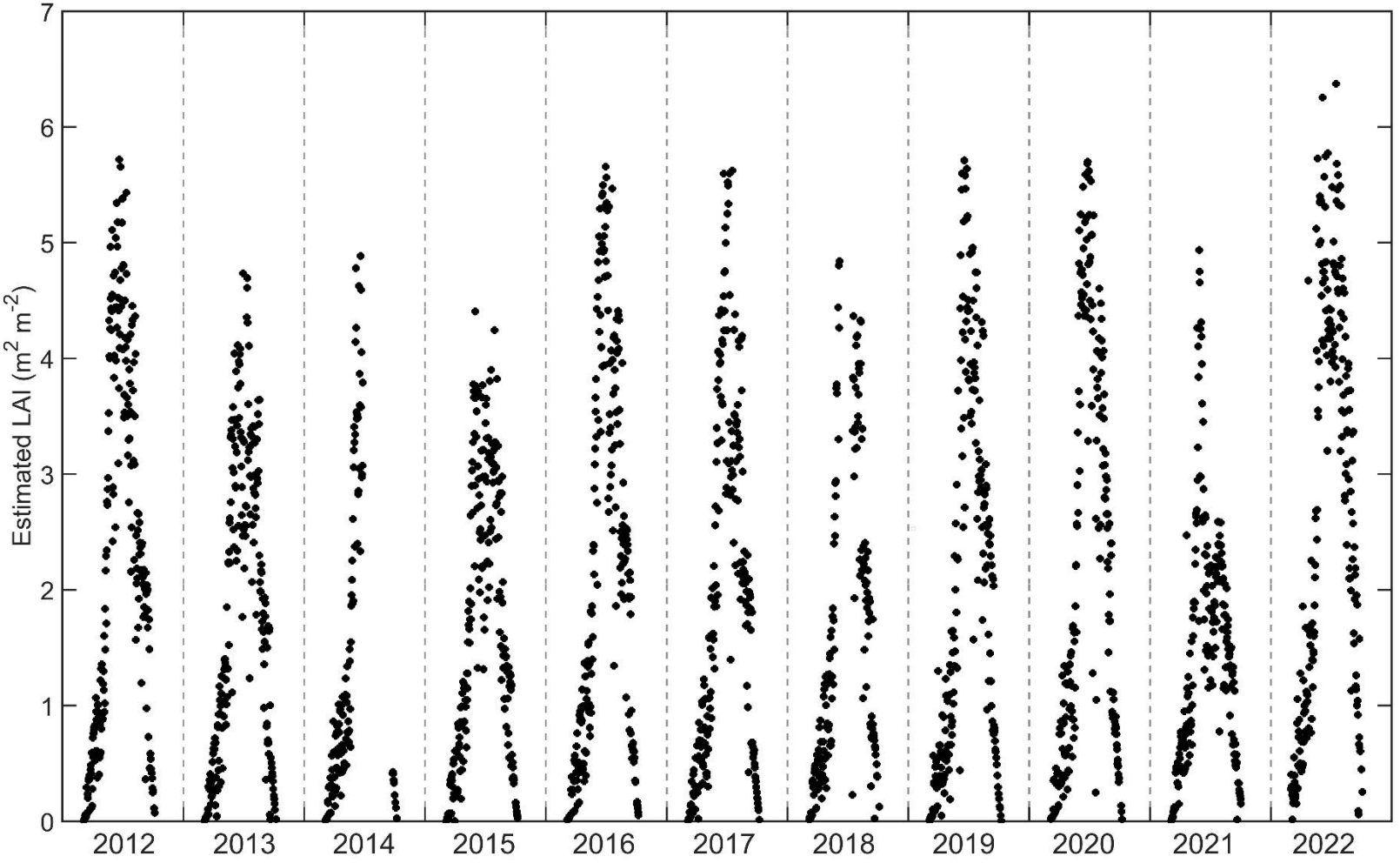

Figure 3b. Daily Leaf Area Index (LAI) estimates for TPD from 2012–2022, calculated using the LAI Simple Method as described by Rogers et al. (2021). The plot displays the maximum LAI value for each day.

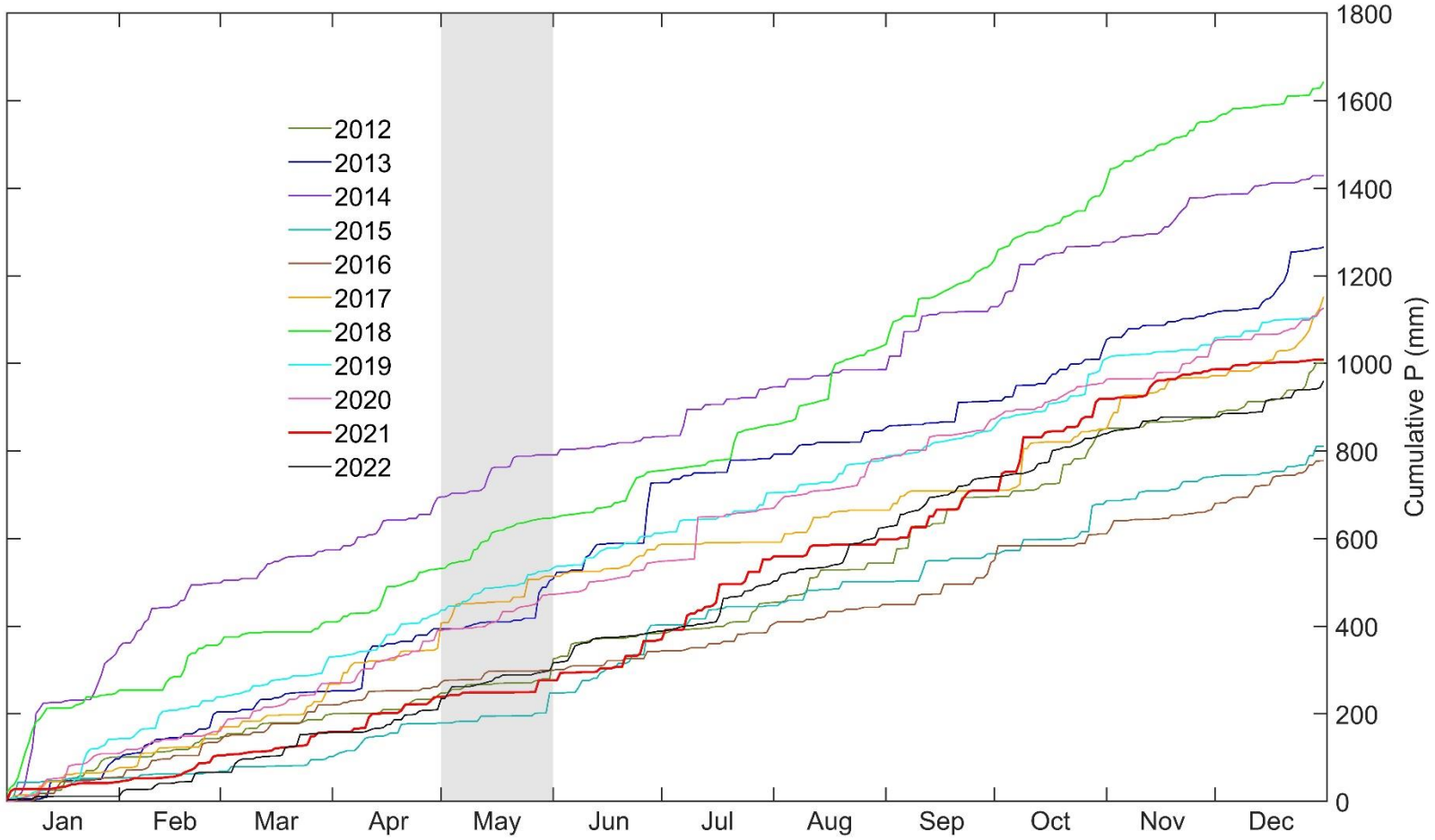

Figure 4. Daily cumulative precipitation (P) from 2012–2022. Grey shading shows early growing season cumulative precipitation levels. In 2021, there was a noticeable dry period during this time.

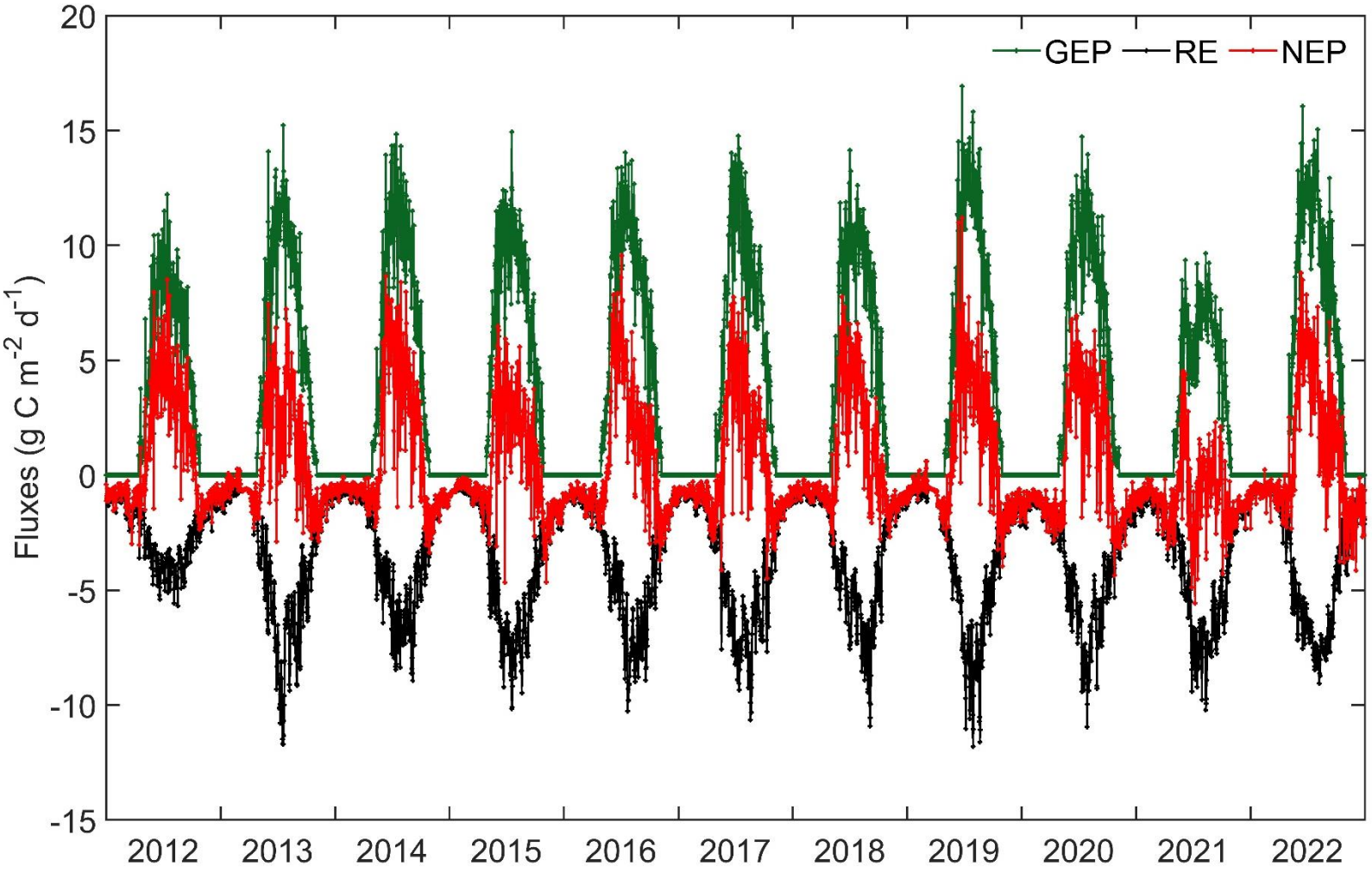

Figure 5. Daily sum of total gross ecosystem productivity (GEP), ecosystem respiration (RE), and net ecosystem productivity (NEP) from 2012–2022.

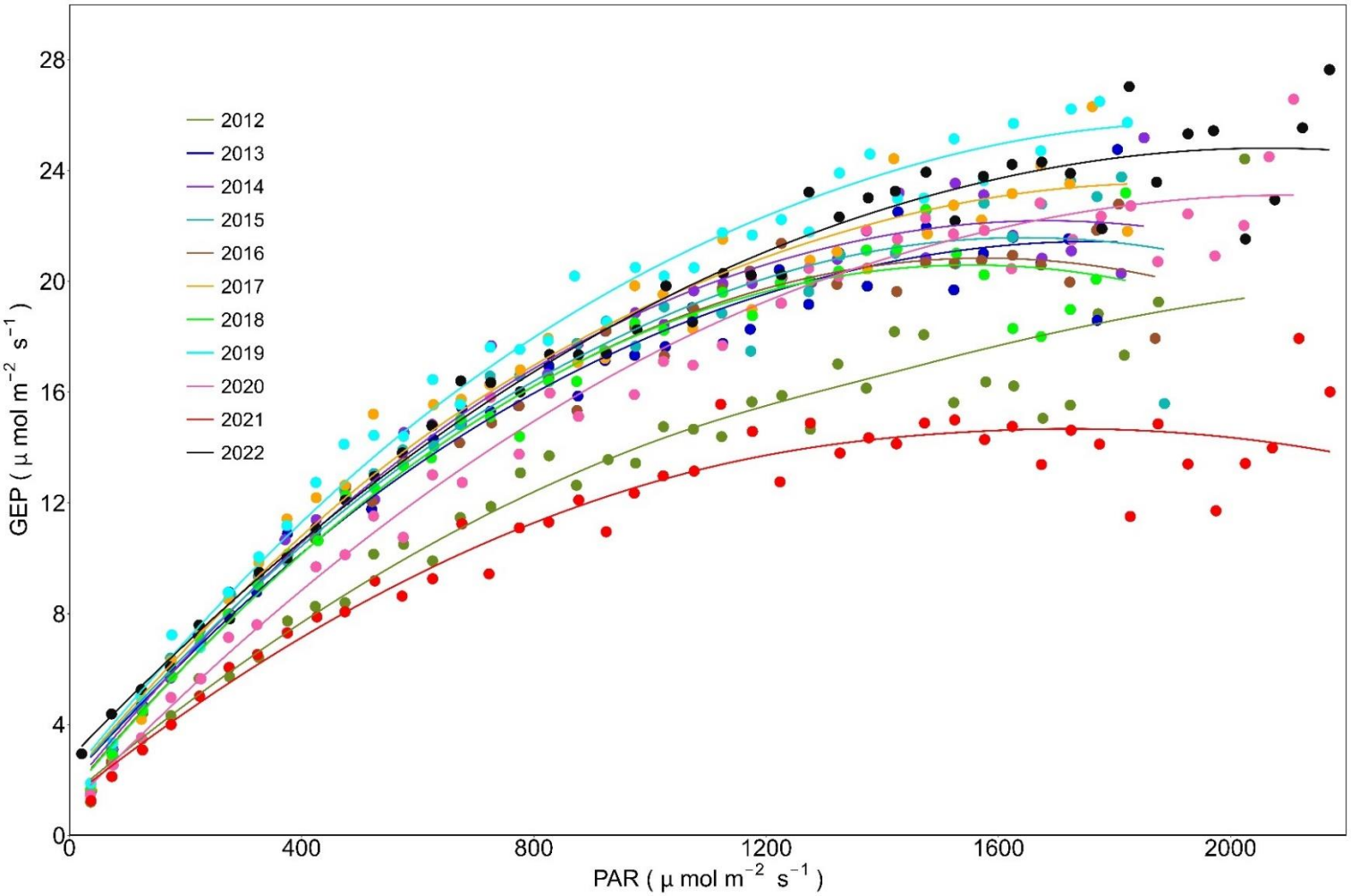

Figure 6. Non-gapfilled, daytime measurements during the growing season, showcasing bin-averaged half-hourly gross ecosystem productivity (GEP) and bin-averaged photosynthetically active radiation (PAR) levels (bin size: 50 µmol m^{-2} s^{-1}) for 2012–2022. The curves represent the fitted hyperbolic model to capture the underlying trend in the data.

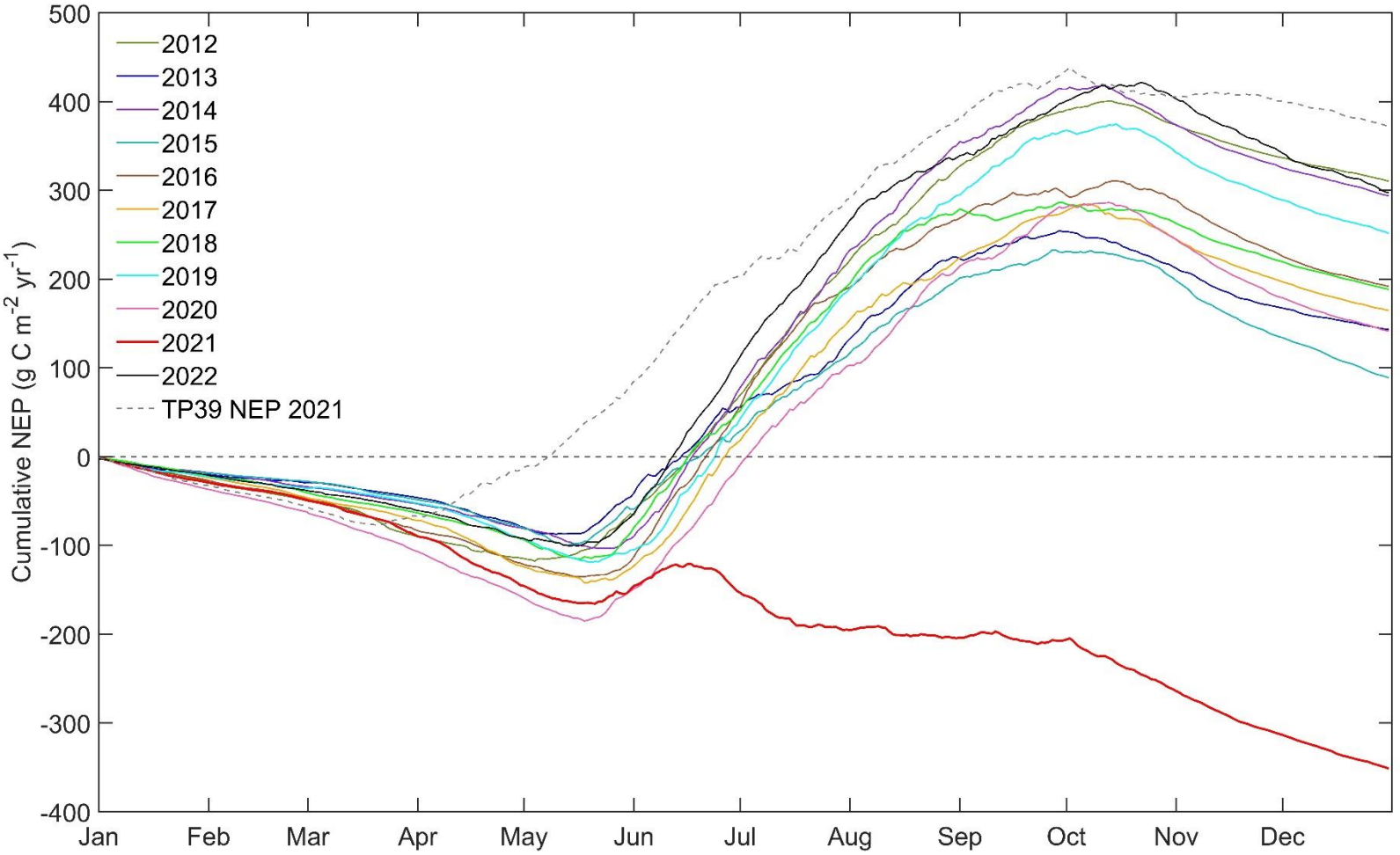

Figure 7. Daily cumulative net ecosystem productivity (NEP) at TPD from 2012–2022. A dotted line representing the cumulative NEP at TP39 has been included for comparison. TP39 is a similarly aged forest of different composition which did not experience defoliation by the spongy moth.